

Hygro-thermal vibration behavior of porous functionally graded nanobeams based on doublet mechanics

U. GUL^{*}), M. AYDOĞDU

*Department of Mechanical Engineering, Trakya University, 22030, Edirne, Turkey,
e-mail^{*}): ufukgul@trakya.edu.tr (corresponding author)*

THIS STUDY DEALS WITH THE VIBRATION RESPONSE of porous functionally graded (FG) nanobeams under hygro-thermal loadings. The FG nanobeam model is developed based on the Euler–Bernoulli beam theory, in which the doublet mechanics is implemented to account for the size effect. The material properties of the FG nanobeam are assumed to vary along the thickness direction of the beam according to the power-law form with the temperature dependent and porosity phases. The approximate Ritz method is employed to obtain the natural frequencies of porous FG nanobeam models for various boundary conditions. The influences of several parameters such as temperature rise, moisture concentration, porosity volume fraction, material gradient index, material length scale parameter and mode number on the free vibration response of the porous FG nanobeams under hygro-thermal environments are examined in detail. It is explicitly shown that the proposed approach can provide accurate frequency results of FG nanobeams as compared to existing studies in open literature. These study's results may be useful for the optimal and safety design of nano-electro-mechanical systems.

Key words: porous functionally graded nanobeams, hygro-thermal loadings, vibration, doublet mechanics, Ritz method.



Copyright © 2024 The Authors

Published by IPPT PAN. This is an open access article under the Creative Commons Attribution License CC BY 4.0 (<https://creativecommons.org/licenses/by/4.0/>).

1. Introduction

THE FUNCTIONALLY GRADED MATERIALS (FGMs) have attracted a great deal of attention due to their advanced material properties, such as high strength, high thermal and corrosive resistances. Recently, with the rapidly development of the nanotechnology field, FGMs in nanoscale have been used in nano-electro-mechanical systems (NEMS) [1–4], atomic force microscopes [5], and sensors [6]. In this context, FG nanobeams are commonly used in NEMS as components of the sensors, transistors, actuators, probes and resonators [7, 8]. Therefore, understanding the mechanical properties of FG nanobeams is very crucial for its practical applications.

It is well-known that the non-classical continuum theories capture the size-dependency of nanostructures and predict accurate results in their static and

dynamic analyses. The most popular size-dependent continuum theories can be regarded as couple stress [9], nonlocal elasticity [10], strain gradient [11], nonlocal strain gradient [12], peridynamics [13], modified couple stress [14] and stress driven integral elasticity [15]. Moreover, another scale-dependent theory is known as doublet mechanics (DM) which has been invented by GRANIK [16]. The main difference of DM from other non-classical continuum theories aforementioned is its direct dependence of the nanostructure of the solid. In DM, the bonding length of the atoms in the structure is taken directly as the material length scale parameter. This proves that scale-dependent parameter is directly related to the atomic structure of the considered material in the DM theory. Micro stresses and strains of the solid are defined by using the Taylor series expansion and then those micro-deformations are transformed to macro stress and strain relations in the DM model. Thus, an efficient connection is established between the discrete mechanics and continuum mechanics. Several papers related to the static and dynamic analyses of FG micro/nano-beams have been published based on the above-mentioned continuum theories. In this context, KE and WANG [17] investigated the dynamic stability of FG microbeams using the modified couple stress theory and the Timoshenko beam theory. REDDY [18] presented the nonlinear bending and buckling analysis of FG Euler–Bernoulli and Timoshenko beams by considering the size effect based on the modified couple stress theory. Static bending and free vibration of FG microbeams have been studied using the modified couple stress theory and various higher order beam theories in [19]. Using the strain gradient theory, AKGÖZ and CİVALEK [20] examined the buckling of size-dependent FG microbeams for different boundary conditions. Also, the shear deformation beam model with new shear correction factors has been developed for FG microbeams by the same authors [21]. RAHMANI and PEDRAM [22] investigated the free vibration of FG nanobeams based on the nonlocal Timoshenko beam theory. The effects of length scale parameter, gradient index and length-to-thickness ratio on the vibration of FG nanobeams have been examined in that paper. Using the DM theory, the free vibration and buckling analyses of FG nanobeams have been investigated in [23, 24]. The Ritz method has been used and vibration and buckling results of FG beams have been obtained for different boundary conditions in these papers. Based on the nonlocal strain gradient theory, nonlinear bending and vibration analyses of size-dependent FG beams have been investigated in [25]. GHANDOURAH *et al.* [26] studied the vibration response of porous FG micro/nanobeams in the framework of the nonlocal couple stress continuum model. The analytical solution has been applied to investigate the vibration characteristics of simply supported FG nanobeams in that paper. In another paper [27], the free vibration analysis of FG porous nanobeams has been examined based on the two-variable trigonometric shear deformation theory. Recently, UZUN and YAYLI [28] have analysed the free vi-

bration response of FG porous nanobeams embedded in the Winkler foundation considering the rotary inertia effect. The bending, buckling and vibration analyses of FG nanobeams reinforced by carbon nanotubes have been studied using the polynomial-exponential integral shear deformable theory in [29].

The common use of FGMs in a high temperature environment causes the important changes in material properties. For instance, when temperature increases, Young's modulus usually decreases in FGMs. Also, during the manufacturing process of FGMs, porosities or micro voids occur in the structure. Thus, to predict the mechanical behaviour of FGMs having porosities and under hygro-thermal environments more accurately, it is necessary to consider the effects of temperature changes and porosities in FG micro/nano-beams. Within this context, EBRAHIMI and SALARI [30] studied the thermal effect on vibration behaviour of FG nanobeams using Eringen's nonlocal elasticity theory. They employed a semi analytical differential transform method in their analysis. In another paper [31], thermal buckling and free vibration analyses of FG nanobeams have been investigated based on the nonlocal Timoshenko beam theory. EBRAHIMI and SALARI [32] developed a nonlocal beam model for the free vibration analysis of FG nanobeams in thermal environments based on the Euler-Bernoulli beam theory. The vibrations results are presented for various boundary conditions in that paper. Thermo-mechanical vibration analysis of FG beams with porosity has been examined in [33]. JOUNEGHANI *et al.* [34] analysed the bending response of FG nanobeams with internal porosity and subjected to a hygro-thermo-mechanical loadings in the framework of the nonlocal elasticity theory. A detailed investigation about the bending response of FG nanobeams was performed by the authors, for the varying power-law index, porosity volume fraction, temperature rise and moisture concentration. JALAEI *et al.* [35] utilized the nonlocal strain gradient model to perform the dynamic instability of the Timoshenko FG nanobeam exposed to a magnetic field in a thermal environment. EBRAHIMI and BARATI [36] developed a unified formulation for vibrational behaviour of FG nanobeams in a hygro-thermal environment. WANG *et al.* [37] researched the hygro-thermal mechanical behaviours of axially FG microbeams based on the refined first-order shear deformation theory. PENNA *et al.* [38] investigated the hygro-thermal vibration of porous FG nanobeams using the local and nonlocal stress gradient theories of elasticity for cantilever and fully clamped nanobeam models. In other study [39], the bending response of porous FG Euler-Bernoulli nanobeams under hygro-thermal loadings has been studied based on the local/nonlocal strain and stress gradient theories. LI *et al.* [40] presented a detailed research about the effects of temperature rise and moisture concentration on the buckling of porous FG nanobeams by using various beam theories. Recently, ÖZMEN *et al.* [41] used the nonlocal strain gradient theory to investigate the thermomechanical vibration and buckling behaviours of FG

porous nanobeams in a magnetic field. Further studies related to the effects of the thermal environment and porosity on the static and dynamic behaviours of FG nanobeams can be found in [42–55].

Although the dynamic analysis of FG nanobeams is being examined by a lot of researchers, studies on the free vibration of porous FG nanobeams considering the hygro-thermal effects are limited. Therefore, there is a strong scientific need to understand the free vibration characteristics of FG nanobeams taking into account the effects of porosity and hygro-thermal environment. Motivated by this fact, the present study investigates the free vibration behaviour of porous FG nanobeams subjected to hygro-thermo-mechanical loads based on the scale-dependent DM theory. Here, the material characteristics of the porous FG beam vary through the beam thickness according to the power-law form and they are temperature-dependent. Also, it is assumed that a linear temperature rise occurs in the thickness direction of the beam. The approximate Ritz method is employed for the vibration analysis of porous FG nanobeams with three combinations of boundary conditions. Application of the Ritz method on the dynamic analysis of the FG beam is simple and reliable and accurate vibration results can be obtained by this method. The Ritz solutions require small degrees of freedom in analysis and have many advantages in handling other parameters, such as simple control parameters of the boundary conditions and the aspect ratios of structures. Moreover, there are different solution methodologies in the open literature to deal with the structural problems wherein the primary (kinematic) or the secondary (kinetic) field variables are assumed to have a series solution form [56–58]. These alternative solution techniques can be also used in the free vibration analysis of FG nanobeams. In the present paper, the influences of the material length scale parameter, porosity volume fraction, temperature rise, moisture concentration, power-law index, mode number and boundary conditions on the vibration response of porous FG nanobeams subjected to hygro-thermo-mechanical loads are examined in detail. The validation is provided for the present results with the results from the existing literature. It is observed that the porosity and hygro-thermal effects change the vibration frequencies of FG nanobeams significantly. The present article can be useful in the design and analysis of NEMs susceptible to hygro-thermal environment and can also provide a valuable source for validating other approximate approaches.

2. Temperature-dependent porous FG nanobeam model

A FG nanobeam model made up of a combination of metal and ceramic subjected to hygro-thermal loads with length L , thickness h and width b , is shown in Fig. 1.

It is assumed that the FG nanobeam has an even porosity distribution

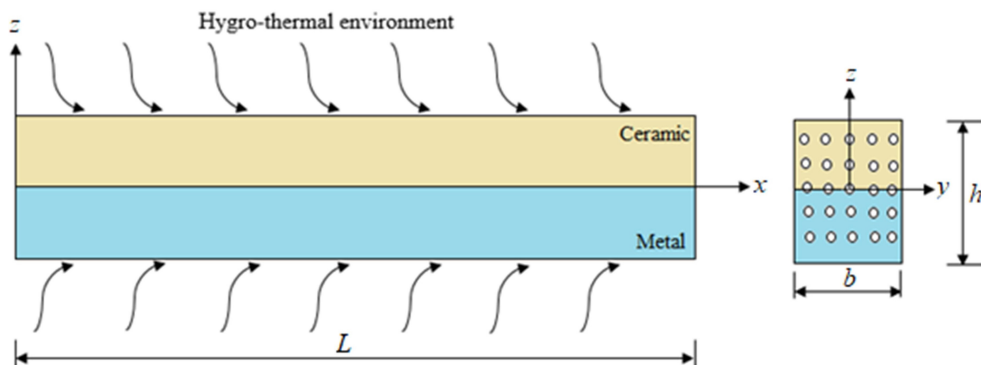


FIG. 1. A porous FG nanobeam in hygro-thermal environment.

through the thickness due to the applied production methods. Accordingly, the mechanical characteristics of the FG nanobeam with the linear uniform porosity distribution can be computed by the following rule of mixture equations:

$$(2.1) \quad P(z) = P_m + (P_c - P_m) \left(\frac{z}{h} + \frac{1}{2} \right)^k - \frac{p}{2} (P_c + P_m),$$

where $P(z)$ is the effective material property change along the thickness (z -axis) of the FG nanobeam, P_m and P_c are the material properties of the metal and ceramic constituents of the FG nanobeam, respectively, k is the power-law index and p is the porosity volume fraction. According to Eq. (2.1), Young's modulus, $E(z)$, density, $\rho(z)$, thermal expansion coefficient, $\gamma(z)$ and moisture expansion coefficient, $\psi(z)$ can be computed as follows:

$$(2.2) \quad E(z) = E_m + (E_c - E_m) \left(\frac{z}{h} + \frac{1}{2} \right)^k - \frac{p}{2} (E_c + E_m),$$

$$(2.3) \quad \rho(z) = \rho_m + (\rho_c - \rho_m) \left(\frac{z}{h} + \frac{1}{2} \right)^k - \frac{p}{2} (\rho_c + \rho_m),$$

$$(2.4) \quad \gamma(z) = \gamma_m + (\gamma_c - \gamma_m) \left(\frac{z}{h} + \frac{1}{2} \right)^k - \frac{p}{2} (\gamma_c + \gamma_m),$$

$$(2.5) \quad \psi(z) = \psi_m + (\psi_c - \psi_m) \left(\frac{z}{h} + \frac{1}{2} \right)^k - \frac{p}{2} (\psi_c + \psi_m).$$

Here, E_m , E_c and ρ_m , ρ_c denote the Young moduli and densities of metal and ceramic, respectively; and γ_m , γ_c and ψ_m , ψ_c , denote the thermal expansion coefficients and moisture expansion coefficients of metal and ceramic materials, respectively. It is noted that all properties of the FG nanobeam are equal to

metal's at the bottom surface where $z = -h/2$, while on the top surface where $z = +h/2$, properties are equal to ceramic's.

The effects of the hygro-thermal environment are considered necessary in more accurately estimating the mechanical behaviour of FGM structures. Thus, the material properties can be defined by a nonlinear temperature-dependent equation [59]:

$$(2.6) \quad P(T) = P_0(P_{-1}T^{-1} + 1 + P_1T + P_2T^2 + P_3T^3),$$

where P_0 , P_{-1} , P_1 , P_2 and P_3 denote the temperature-dependent coefficients. In this paper, linear temperature rise ($T(z)$) and linear moisture concentration ($C(z)$) are considered between the bottom ($z = -h/2$) and top ($z = +h/2$) surfaces of the nanobeam cross-section:

$$(2.7) \quad T(z) = T_m + \Delta T \left(\frac{z}{h} + \frac{1}{2} \right),$$

$$(2.8) \quad C(z) = C_m + \Delta C \left(\frac{z}{h} + \frac{1}{2} \right),$$

where

$$(2.9) \quad \Delta T = T_c - T_m,$$

$$(2.10) \quad \Delta C = C_c - C_m.$$

Here, T_c , C_c and T_m , C_m are the values of the temperature and moisture concentration at the top and bottom surface, respectively, ΔT and ΔC are the temperature and moisture concentration rise, respectively. The temperature-dependent coefficients of material phases for metal (SuS_3O_4) and ceramic (Si_3N_4) are given in Table 1 [60].

TABLE 1. Temperature-dependent coefficients for the constituents of FG beam.

Material	Properties	P_{-1}	P_0	P_1	P_2	P_3
Si_3N_4	E_c (GPa)	0	348.43	-0.0003070	2.160E-07	-8.946E-11
	ρ_c [kg/m ³]	0	2370	0	0	0
	γ_c [K ⁻¹]	0	5.8723E-06	0.0009095	0	0
	ψ_c (wt.% H ₂ O) ⁻¹	0	0	0	0	0
SuS_3O_4	E_m (GPa)	0	201.04	0.0003079	-6.534E-07	0
	ρ_m [kg/m ³]	0	8166	0	0	0
	γ_m [K ⁻¹]	0	12.330E-06	0.0008086	0	0
	ψ_m (wt.% H ₂ O) ⁻¹	0	0.0005	0	0	0

3. Doublet mechanics formulation

The doublet mechanics (DM) theory considers two adjacent atoms or nodes as a doublet and incorporates a material length scale parameter to account for their distance from each other. This material length scale parameter in DM is simply demonstrated in Fig. 2.

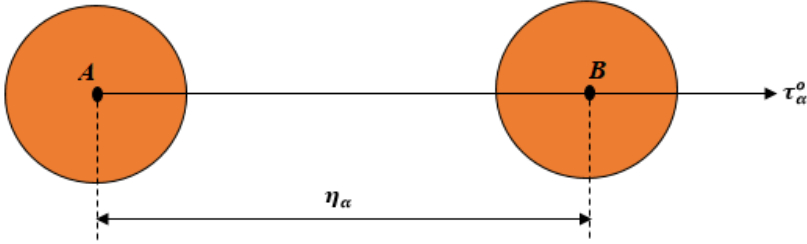


FIG. 2. A doublet geometry in DM theory.

Then, the increment (Δu_α) in the stretching displacement of doublet α is defined as [61]:

$$(3.1) \quad \Delta u_\alpha = \sum_{\chi=1}^M \frac{(\eta_\alpha)^\chi}{\chi!} \tau_{\alpha k_1}^o \cdots \tau_{\alpha k_\chi}^o \frac{\partial^\chi u_i}{\partial \chi_{k_1} \cdots \partial \chi_{k_\chi}}.$$

Here, k_1, k_2, \dots, k_χ are equal to 1, 2 and 3 in the Cartesian coordinate and in this paper 1, 2 and 3 are x, y and z axes, respectively. Any two nodes in a solid are called as a doublet and distance between two nodes is called as a material length scale in the DM theory [61]. These nodes (atoms) are located at certain finite distances (bond length) of the order of a few angstroms to nanometers (for example the carbon-carbon bond length is 0.1421 nm). For the present problem, the material length scale parameter of FG nanobeams, $\eta = 0.1421$ nm is taken into account in the calculations; τ_α^o is the unit vector in the direction of α -th node, and M is the number of terms in the Taylor series expansion. The stretching micro-strain (ϵ_α) in terms of the unit vector in α -direction can be defined as [61]:

$$(3.2) \quad \epsilon_\alpha = \tau_{\alpha i}^o \sum_{\chi=1}^M \frac{(\eta_\alpha)^\chi}{\chi!} \tau_{\alpha k_1}^o \cdots \tau_{\alpha k_\chi}^o \frac{\partial^\chi u_i}{\partial \chi_{k_1} \cdots \partial \chi_{k_\chi}}.$$

For the present paper, $M = 3$ terms of the Taylor series is taken into account in the DM theory. It is known from the previous works that $M = 3$ terms of

the Taylor series can provide satisfactory results for the DM theory [62, 63]. Therefore, using this assumption, the stretching micro-strain is obtained as:

$$(3.3) \quad \epsilon_\alpha = \tau_{\alpha i}^o \tau_{\alpha j}^o \frac{\partial u_i}{\partial x_j} + \tau_{\alpha i}^o \frac{\eta_\alpha}{2} \tau_{\alpha j}^o \tau_{\alpha k}^o \frac{\partial^2 u_i}{\partial x_j \partial x_k} + \tau_{\alpha i}^o \frac{\eta_\alpha^2}{6} \tau_{\alpha j}^o \tau_{\alpha k}^o \tau_{\alpha l}^o \frac{\partial^3 u_i}{\partial x_j \partial x_k \partial x_l}.$$

The relation between micro-stress and micro-strain is [61]:

$$(3.4) \quad p_\alpha = \sum_\beta C_{\alpha\beta} \epsilon_\beta,$$

where $C_{\alpha\beta}$ is the micro-moduli of elasticity of doublet and can be defined as a constant (C_0) with the assumption of the plane stress condition [53]:

$$(3.5) \quad C_0 = \frac{4}{9} \mu \frac{7\lambda + 10\mu}{\lambda + 2\mu}.$$

Lamé's constants, λ and μ and C_0 are defined with the assumption of the plane stress condition and putting $\nu = 1/3$, one obtains [62]:

$$(3.6) \quad \begin{aligned} \lambda &= \frac{\nu E}{(1 + \nu)(1 - 2\nu)}, & \mu &= G = \frac{E}{2(1 + \nu)}, \\ \lambda &= 2\mu, & C_0 &= \frac{8\mu}{3} = E, \end{aligned}$$

where E and ν represent the elasticity modulus Poisson ratio, respectively. Then, the stretching micro-strain and micro-stress are achieved by:

$$(3.7) \quad \epsilon_\alpha = \tau_{\alpha i}^o \tau_{\alpha j}^o \frac{\partial u_i}{\partial x_j} + \tau_{\alpha i}^o \frac{\eta_\alpha}{2} \tau_{\alpha j}^o \tau_{\alpha k}^o \frac{\partial^2 u_i}{\partial x_j \partial x_k} + \tau_{\alpha i}^o \frac{\eta_\alpha^2}{6} \tau_{\alpha j}^o \tau_{\alpha k}^o \tau_{\alpha l}^o \frac{\partial^3 u_i}{\partial x_j \partial x_k \partial x_l},$$

$$(3.8) \quad p_\alpha = C_0 \tau_{\alpha m}^o \tau_{\alpha n}^o \left(\epsilon_{mn} + \frac{1}{2} \eta_\alpha \tau_{\alpha s}^o \frac{\partial \epsilon_{mn}}{\partial x_s} + \frac{1}{6} \eta_\alpha^2 \tau_{\alpha t}^o \tau_{\alpha s}^o \frac{\partial^2 \epsilon_{mn}}{\partial x_t \partial x_s} \right).$$

The stretching macro-stress relation can be determined for the three-dimensional formulations as follows [63]:

$$(3.9) \quad \sigma_{k_1 i}^{(M)} = \sum_{\alpha=1}^M \tau_{\alpha k_1}^o \sum_{\chi=1}^M (-1)^{\chi+1} \left[\frac{(\eta_\alpha)^{\chi-1}}{\chi!} \tau_{\alpha k_2}^o \dots \tau_{\alpha k_\chi}^o \frac{\partial^{\chi-1} p_{\alpha i}}{\partial \chi_{k_2} \dots \partial \chi_{k_\chi}} \right].$$

By putting $M = 3$ in Eq. (3.9) leads to

$$(3.10) \quad \sigma_{ij} = \sum_{\alpha=1}^M C_0 \tau_{\alpha i}^o \tau_{\alpha j}^o \tau_{\alpha m}^o \tau_{\alpha n}^o \left[\epsilon_{mn} + \frac{\eta_\alpha^2}{12} \tau_{\alpha t}^o \tau_{\alpha s}^o \frac{\partial^2 \epsilon_{mn}}{\partial x_t \partial x_s} \right].$$

The unit vectors $\vec{\tau}_{ij}^o$ which are the cosines of the angles between the micro-stresses and the Cartesian coordinates and can be calculated according to Fig. 3 as follows:

$$(3.11) \quad \tau_{ij} = \begin{bmatrix} \cos \theta & \cos 90^\circ & \sin \theta \\ -\sin(30^\circ - \theta) & \cos 90^\circ & -\cos(30^\circ - \theta) \\ -\cos(60^\circ - \theta) & \cos 90^\circ & \sin(60^\circ - \theta) \end{bmatrix}.$$

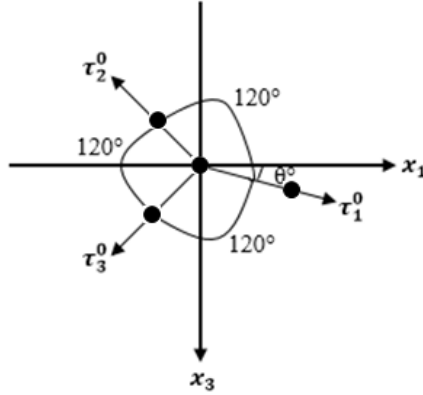


FIG. 3. Configuration of three doublets with equal angles.

For the present problem, the zigzag nanobeam model is considered. Thus, the angle of atomic structure with beam's axial direction θ is taken as 0° for the zigzag structure. By putting $\theta = 0^\circ$ in Eq. (3.11) the following is obtained:

$$(3.12) \quad \tau_{ij} = \begin{bmatrix} 1 & 0 & 0 \\ -1/2 & 0 & -\sqrt{3}/2 \\ -1/2 & 0 & \sqrt{3}/2 \end{bmatrix}.$$

By substituting Eq. (3.12) into Eq. (3.10) and assuming $C_0 = E$ for the plane stress condition, the stress-strain relation can be obtained for the zigzag model as follows:

$$(3.13) \quad \sigma_{xx} = E \left(\varepsilon_{xx} + \frac{\eta_\alpha^2}{12} \frac{\partial^2 \varepsilon_{xx}}{\partial x^2} + \frac{\eta_\alpha^2}{32} \frac{\partial^2 \varepsilon_{xz}}{\partial x \partial z} \right).$$

Considering only the longitudinal strain in Eq. (3.13) yields:

$$(3.14) \quad \sigma_{xx} = E \left(\varepsilon_{xx} + \frac{\eta^2}{12} \frac{\partial^2 \varepsilon_{xx}}{\partial x^2} \right).$$

It is noted that $\frac{\eta^2}{12}$ term in Eq. (3.14) represents the material length scale parameter of the DM theory for the zigzag structure.

4. The DM model for FG nanobeam

Considering the DM theory, the strain energy (U_s) of a FG nanobeam can be written as:

$$(4.1) \quad U_s = \frac{1}{2} \int_A \int_0^L [\tau_x \cdot \varepsilon_x - \mu_x \cdot \nabla \varepsilon_x] dx dA,$$

where τ_x is the macro stress with respect to the x -axis, ε_x is the normal strain ($\varepsilon_x = -y \frac{d^2 w}{dx^2}$), A is the cross-sectional area and L is the length of the nanobeam. τ_x , $\nabla \varepsilon_x$ and μ_x are computed as:

$$(4.2) \quad \nabla \varepsilon_x = d\varepsilon_x/dx, \quad \tau_x = E(z)\varepsilon_x, \quad \mu_x = \frac{\eta^2}{12} E(z) \frac{d\varepsilon_x}{dx}.$$

Substituting Eq. (4.2) into Eq. (4.1) yields:

$$(4.3) \quad U_s = \frac{1}{2} \int_0^L E(z) I \left[\left(\frac{\partial^2 w}{\partial x^2} \right)^2 - \frac{\eta^2}{12} \left(\frac{\partial^3 w}{\partial x^3} \right)^2 \right] dx.$$

In which I is the moment of inertia of the rectangular beam cross-section is equal to $I = bh^3/12$. The kinetic energy (T) of the FG nanobeam is defined as:

$$(4.4) \quad T = \frac{1}{2} \int_0^L \rho(z) A \left(\frac{\partial w}{\partial t} \right)^2 dx.$$

It is assumed that the considered FG nanobeam which has been in hygro-thermal environment for a long period of time and linear changes of temperature and moisture are taken into consideration. In this context, the work done by applied forces (W_e) due to the temperature and moisture change can be written in the following form:

$$(4.5) \quad W_e = -\frac{1}{2} \int_0^L (N^T + N^C) \left(\frac{\partial w}{\partial x} \right)^2 dx,$$

where N^T and N^C are the hygro-thermal axial force resultants due to temperature and moisture change, respectively, defined as follow:

$$(4.6) \quad N^T = b \int_{-h/2}^{h/2} E(z, T) \gamma(z, T) \Delta T dz, \quad N^C = b \int_{-h/2}^{h/2} E(z, T) \psi(z, T) \Delta C dz,$$

where b is the width of the beam.

5. Ritz solution for FG nanobeam model

Assuming the harmonic vibration in a FG nanobeam, $w(x, t)$ can be defined as:

$$(5.1) \quad w(x, t) = W(x) \cos \omega t,$$

where $W(x)$ is the amplitude of the transverse displacement and ω is the natural frequency of the FG nanobeam. According to the Ritz method, the displacement constituent can be expressed as:

$$(5.2) \quad W(x) = \sum_{i=1}^N D_i \zeta_i(x).$$

Here, D_i are arbitrary coefficients and $\zeta_i(x)$ is an admissible function that satisfies at least geometric boundary conditions but not necessary for satisfying the natural boundary conditions of the beam. For the present study, simply supported-simply supported (S-S), clamped-clamped (C-C) and clamped-simply supported (C-S) boundary conditions of the FG nanobeam are considered. Accordingly, the geometric and natural boundary conditions of the beam are defined as [64]:

For the simply supported boundary condition we use:

$$(5.3a) \quad \begin{aligned} w(x, t) &= 0, \\ EI \left[\left(\frac{\partial^2 w(x, t)}{\partial x^2} \right) + \frac{\eta^2}{12} \left(\frac{\partial^4 w(x)}{\partial x^4} \right) \right] &= 0, \\ \frac{\partial^2 w(x)}{\partial x^2} &= 0 \quad \text{at } x = 0, L. \end{aligned}$$

For the clamped boundary condition we use:

$$(5.3b) \quad \begin{aligned} w(x) &= 0, \\ \frac{\partial w(x)}{\partial x} &= 0, \\ \frac{\partial^2 w(x)}{\partial x^2} &= 0 \quad \text{at } x = 0, L. \end{aligned}$$

The admissible function can be assumed in the following form:

$$(5.4) \quad \zeta_i(x) = x^i, \quad i = 1, 2, \dots, N.$$

The dimensionless form of the algebraic polynomial (x^i) can be defined as:

$$(5.5) \quad x^i = \bar{x}^i (\bar{x} - 1)^d, \quad \bar{x} = \frac{x}{L}.$$

Here, the values of d in Eq. (5.5) are chosen $d = 1$ and 2 for the simply supported and clamped edges, respectively. It should be noted that the admissible function is compatible with the geometric boundary conditions given in Eq. (5.2). According to the Ritz method, the maximum potential energy (U_{\max}) and kinetic energy (T_{\max}) are calculated by inserting Eq. (5.1) into Eqs. (4.3)–(4.5) and setting $\cos \omega t$ equal to 1:

$$(5.6) \quad U_{\max} = \frac{1}{2} \int_0^L E(z, T) I \left[\left(\frac{\partial^2 W}{\partial x^2} \right)^2 - \frac{\eta^2}{12} \left(\frac{\partial^3 W}{\partial x^3} \right)^2 \right] dx$$

$$- \frac{1}{2} \int_0^L (N^T + N^C) \left(\frac{\partial W}{\partial x} \right)^2 dx,$$

$$(5.7) \quad T_{\max} = \frac{1}{2} \int_0^L \rho(z, T) A \omega^2 (W)^2 dx.$$

Then, Langrangian functional (L) can be expressed as:

$$(5.8) \quad L = U_{\max} - T_{\max}.$$

Finally, by minimization of Eq. (5.8) with respect to undetermined coefficients (D_i), the general eigenvalue problem is:

$$(5.9) \quad \frac{\partial L}{\partial D_i} = 0.$$

Equation (5.9) gives $I \times I$ simultaneous, linear, and homogeneous equations as below

$$(5.10) \quad ([K] - \Omega^2[M])\{\Delta\} = 0.$$

The size of Eq. (5.10) is equal to the sum of the number of undetermined coefficients (D_i). Here, $[K]$ and $[M]$ represent the stiffness and mass matrices, respectively, $\{\Delta\}$ represents the column vector of the undetermined coefficients D_i , and Ω represents the dimensionless frequency parameter of porous FG nanobeams under hygro-thermal loadings based on DM and it is defined as:

$$(5.11) \quad \Omega = \omega L^2 \sqrt{\rho_c A / E_c I}.$$

6. Numerical results and discussions

In this section, the hygro-thermal mechanical vibration response of the FG porous Euler–Bernoulli nanobeams is investigated using the size-dependent DM theory. The analysis has been conducted employing the usefulness of the Ritz

method for different boundary conditions such as S-S, C-C and C-S. The FG nanobeam model is composed of Silicon nitride (Si_3N_4) and Steel (SuS_3O_4) where its properties are presented in Table 1. The top surface of the beam is pure Steel (SuS_3O_4) while the bottom surface of the beam is pure Silicon nitride (Si_3N_4).

In Table 2, the convergence study of the Ritz method is demonstrated for the first three dimensionless natural frequency of the porous FG beam under a hygro-thermal environment with various boundary conditions. It is observed that the first three natural frequencies converged to a value with good precision for $N = 8$ iterations in the Ritz method for all given boundary conditions. Therefore, $N = 8$ terms can be used in the Ritz method to calculate the natural frequencies of the FG nanobeam for the present study.

TABLE 2. Convergence of the first three dimensionless frequency parameters for different boundary conditions ($L/h = 20, k = 1, p = 0.2, \Delta T = 40 \text{ [K]}, \Delta C = 1$).

N	S-S		C-C		C-S	
	$\eta = 0$	$\eta = 0.1421 \text{ nm}$	$\eta = 0$	$\eta = 0.1421 \text{ nm}$	$\eta = 0$	$\eta = 0.1421 \text{ nm}$
First dimensionless frequency (Ω_1)						
3	5.4637	5.4635	13.3213	13.3199	8.9936	8.9930
5	5.4617	5.4613	13.3210	13.3196	8.9830	8.9825
6	5.4617	5.4613	13.3210	13.3196	8.9830	8.9824
7	5.4617	5.4613	13.3210	13.3196	8.9830	8.9824
8	5.4617	5.4613	13.3210	13.3196	8.9830	8.9824
Second dimensionless frequency (Ω_2)						
3	30.0981	30.0973	37.9134	37.8998	30.4244	30.4174
5	23.5935	23.5907	37.1373	37.1291	29.9523	29.9479
6	23.4907	23.4887	37.1247	37.1160	29.9459	29.9415
7	23.4907	23.4887	37.1247	37.1160	29.9459	29.9390
8	23.4907	23.4887	37.1247	37.1160	29.9459	29.9390
Third dimensionless frequency (Ω_3)						
3	79.7719	79.7637	77.2539	77.1930	109.8454	109.8222
5	54.4337	54.4165	73.2557	73.2285	64.7097	64.6784
6	54.4337	54.4165	73.2557	73.2285	63.0369	63.01957
7	53.5231	53.5132	73.1174	73.0880	62.9802	62.9629
8	53.5231	53.5132	73.1174	73.0880	62.9408	62.9225

To evaluate the accuracy and reliability of the present approach, a comparison study with the dimensionless frequencies of FG beams in thermal environments for various boundary conditions and power-law indexes are given in Tables 3 and 4. Using the same material properties given in [30], the first di-

TABLE 3. Comparison of the first dimensionless frequency ($\Omega = \omega L^2 \sqrt{\rho_c A / E_c I}$) of functionally graded beams in thermal environment ($L/h = 20$, $\eta = 0$).

Boundary condition	k	Ω_1	$\Delta T = 20$ [K]	$\Delta T = 40$ [K]	$\Delta T = 80$ [K]
S-S	0.1	Present	8.5204	8.3433	7.9771
		[30]	8.4633	8.2780	7.8794
	0.2	Present	7.8143	7.6422	7.2858
		[30]	7.7346	7.5558	7.1710
0.5	Present	6.6329	6.4670	6.1217	
	[30]	6.5412	6.3715	6.0061	
1	Present	5.7621	5.5981	5.2549	
	[30]	5.7110	5.5466	5.1925	
C-C	0.1	Present	19.7650	19.6704	19.4799
		[30]	19.6398	19.5436	19.3420
	0.2	Present	18.1527	18.0610	17.8762
		[30]	17.9776	17.8869	17.6968
0.5	Present	15.4588	15.3709	15.1933	
	[30]	15.2580	15.1759	15.0040	
1	Present	13.4781	13.3915	13.2166	
	[30]	13.3671	13.2905	13.1304	
C-S	0.1	Present	13.5247	13.3951	13.1317
		[30]	13.4380	13.3037	13.0201
	0.2	Present	12.4162	12.2904	12.0346
		[30]	12.2947	12.1663	11.8951
0.5	Present	10.5632	10.4423	10.1960	
	[30]	10.4238	10.4238	10.0515	
1	Present	9.1998	9.0807	8.8374	
	[30]	9.1227	9.0082	8.7674	

dimensionless frequencies of FG beams in a thermal environment predicted by the present method are compared to findings of the analytical method [30] in Table 3. It is seen that the current method's results are in good agreement with that reported in [30]. The difference between the current method's results and the results of [30] is due to the solution methods. The first dimensionless frequency results are obtained by using the approximate Ritz method in the present study, whereas the first dimensionless frequency results of FG beams are obtained by the analytical solution method in [30]. It is seen that the highest difference between two methods is approximately 1.92% in Table 3. When the analytical solution is compared with the approximate Ritz solution, it can be said that this difference is acceptable. As it is similar to the previous compar-

TABLE 4. Comparison of the first three dimensionless frequencies ($\Omega = \omega L^2 \sqrt{\rho_c A / E_c I}$) of functionally graded beams in thermal environment for various boundary conditions ($L/h = 20, \eta = 0$).

Boundary condition	k	Ω_i	$\Delta T = 0$		$\Delta T = 20$ [K]		$\Delta T = 40$ [K]	
			Present	[32]	Present	[32]	Present	[32]
S-S	0	$i = 1$	9.8696	9.8594	9.6068	9.5065	9.4275	9.1374
		$i = 2$	39.4784	39.3171	39.2182	38.9700	39.0438	38.6173
		$i = 3$	88.8482	88.0158	88.5885	87.6713	88.4150	87.3231
	0.2	$i = 1$	8.7683	8.6845	8.4999	8.3092	8.3187	7.9105
		$i = 2$	35.0732	34.6263	34.8079	34.2584	34.6324	33.8792
		$i = 3$	78.9340	77.4947	78.6693	77.1298	78.4948	76.7528
	1	$i = 1$	7.1281	7.0638	6.8466	6.6661	6.6557	6.2332
		$i = 2$	28.5123	28.1627	28.2351	27.7749	28.0519	27.3676
		$i = 3$	64.1684	63.0229	63.8920	62.6387	63.7102	62.2303
C-C	0	$i = 1$	22.3732	22.3447	22.2301	22.1532	22.1342	21.9585
		$i = 2$	61.6728	61.3790	61.4788	61.1205	61.3492	60.8590
		$i = 3$	120.9054	119.6770	120.6931	119.3950	120.5513	119.1110
	0.2	$i = 1$	19.8767	19.6819	19.7308	19.4789	19.6342	19.2695
		$i = 2$	54.7910	54.0567	54.5932	53.7827	54.4628	53.4998
		$i = 3$	107.4141	105.3750	107.1977	105.0770	107.0552	104.7670
	1	$i = 1$	16.1585	16.0094	16.0060	15.7954	15.9052	15.5703
		$i = 2$	44.5417	43.9727	44.3352	43.6841	44.1993	43.3779
		$i = 3$	87.3210	85.7255	87.0950	85.4118	86.9466	85.0712
C-S	0	$i = 1$	15.4178	15.3997	15.2229	15.1386	15.0914	14.8707
		$i = 2$	49.9638	49.7431	49.7407	49.4456	49.5914	49.1442
		$i = 3$	104.2469	103.2410	104.0127	102.9310	103.8563	102.6170
	0.2	$i = 1$	13.6974	13.5647	13.4985	13.2874	13.3661	12.9994
		$i = 2$	44.3886	43.8094	44.1611	43.4941	44.0109	43.1693
		$i = 3$	92.6144	90.9059	92.3757	90.5771	92.2184	90.2361
	1	$i = 1$	11.1352	11.0336	10.9271	10.7409	10.7884	10.4310
		$i = 2$	36.0852	35.6368	35.8475	35.3046	35.6909	34.9547
		$i = 3$	75.2898	73.9537	75.0405	73.6074	74.8767	73.2359

ison study, the current method’s results agree well with the results presented by EBRAHIMI and SALARI [32] for the first three dimensionless frequencies and given boundary conditions. The acceptable difference between the results of the current study and [32] is due to the Ritz method used in this study, which gives an approximate solution.

After validation of the current method, in Tables 5–7, the variations of natural frequencies of hygro-thermo-mechanical vibration of porous FG nanobeams

with temperature rise, moisture concentration, porosity volume fraction, power-law index, mode number and boundary conditions are presented for DM and the classical elasticity theory ($\eta = 0$) at the constant slenderness ratio ($L/h = 20$). It can be observed from the results of Tables 5–7 that the dimensionless frequencies predicted by the DM ($\eta = 0.1421$ nm) theory are lower than the dimensionless frequencies obtained by the classical elasticity theory ($\eta = 0$) for all given boundary conditions. The difference between two theories is more pronounced for higher modes of vibration. These results indicate that DM predicts softening material behaviour compared to the classical elasticity theory and the material length scale parameter in DM becomes more significant in higher modes. In addition, it is seen that the changes of the temperature and moisture concentrations have considerable influences on the vibration of the porous FG nanobeams. When the temperature and moisture concentrations increase, the natural frequencies decrease for both DM and classical elasticity theories. This is due to the decrease in the total stiffness of the FG nanobeam with temperature and moisture concentration rises. Rises in temperature and moisture yield increasing compressive forces, leading to the reduction in the rigidity of the beam. The dimensionless natural frequencies decrease with increasing the power-law index. That is

TABLE 5A. The first dimensionless frequency ($\Omega = \sqrt[4]{\rho_c A \omega^2 L^4 / E_c I}$) of porous functionally graded nanobeams under a hygro-thermal environment for S-S boundary condition ($L/h=20$).

η [nm]	ΔC	p	$\Delta T = 0$		$\Delta T = 40$ [K]		$\Delta T = 80$ [K]	
			$k = 0.5$	$k = 2$	$k = 0.5$	$k = 2$	$k = 0.5$	$k = 2$
0	0	0	6.8781	5.3162	6.4670	4.9969	6.1217	4.6639
		0.1	6.9915	5.2482	6.6260	4.9647	6.3220	4.6558
		0.3	7.3384	5.0617	7.0644	4.8494	6.8412	4.6273
	1	0	6.6610	4.9391	6.2356	4.8219	5.8767	4.5139
		0.1	6.8169	4.9134	6.4415	4.8120	6.1283	4.5011
		0.3	7.2527	4.8130	6.9753	4.7413	6.7491	4.4675
	2	0	6.5741	4.7620	6.1427	4.6544	5.7780	4.3976
		0.1	6.7525	4.7591	6.3733	4.6404	6.0566	4.3321
		0.3	7.2352	4.7041	6.9571	4.6307	6.7303	4.2709
0.1421	0	0	6.8780	5.3161	6.4668	4.9968	6.1215	4.6638
		0.1	6.9914	5.2481	6.6258	4.9646	6.3218	4.6557
		0.3	7.3383	5.0616	7.0643	4.8493	6.8410	4.6272
	1	0	6.6609	4.9390	6.2354	4.8218	5.8766	4.5138
		0.1	6.8167	4.9133	6.4413	4.8119	6.1281	4.5010
		0.3	7.2526	4.8129	6.9752	4.7412	6.7490	4.4674
	2	0	6.5740	4.7619	6.1425	4.6542	5.7779	4.3975
		0.1	6.7523	4.7590	6.3731	4.6402	6.0564	4.3320
		0.3	7.2350	4.7039	6.9569	4.6305	6.7301	4.2707

TABLE 5B. The second dimensionless frequency ($\Omega = \sqrt[4]{\rho_c A \omega^2 L^4 / E_c I}$) of porous functionally graded nanobeams under a hygro-thermal environment for S-S boundary condition ($L/h = 20$).

η [nm]	ΔC	p	$\Delta T = 0$		$\Delta T = 40$ [K]		$\Delta T = 80$ [K]	
			$k = 0.5$	$k = 2$	$k = 0.5$	$k = 2$	$k = 0.5$	$k = 2$
0	0	0	27.5126	21.2648	27.1107	20.8715	26.7882	20.5535
		0.1	27.9661	20.9930	27.6078	20.6427	27.3212	20.3602
		0.3	29.3538	20.2468	29.0837	19.9831	28.8694	19.7713
	1	0	27.2981	20.8980	26.8931	20.4976	26.5678	20.1738
		0.1	27.7931	20.6663	27.4326	20.3104	27.1441	20.0232
		0.3	29.2685	20.0028	28.9976	19.7357	28.7826	19.5213
	2	0	27.2137	20.7329	26.8074	20.3293	26.4811	20.0027
		0.1	27.7302	20.5214	27.3688	20.1629	27.0796	19.8736
		0.3	29.2511	19.8988	28.9800	19.6304	28.7650	19.4148
0.1421	0	0	27.5103	21.2630	27.1084	20.8697	26.7858	20.5517
		0.1	27.9638	20.9913	27.6055	20.6409	27.3188	20.3584
		0.3	29.3514	20.2451	29.0812	19.9813	28.8669	19.7696
	1	0	27.2958	20.8962	26.8907	20.4957	26.5655	20.1719
		0.1	27.7908	20.6645	27.4302	20.3086	27.1417	20.0214
		0.3	29.2660	20.0011	28.9951	19.7340	28.7801	19.5196
	2	0	27.2113	20.7311	26.8050	20.3274	26.4787	20.0008
		0.1	27.7278	20.5196	27.3664	20.1611	27.0772	19.8717
		0.3	29.2487	19.8971	28.9775	19.6287	28.7625	19.4131

TABLE 5C. The third dimensionless frequency ($\Omega = \sqrt[4]{\rho_c A \omega^2 L^4 / E_c I}$) of porous functionally graded nanobeams under a hygro-thermal environment for S-S boundary condition ($L/h = 20$).

η [nm]	ΔC	p	$\Delta T = 0$		$\Delta T = 40$ [K]		$\Delta T = 80$ [K]	
			$k = 0.5$	$k = 2$	$k = 0.5$	$k = 2$	$k = 0.5$	$k = 2$
0	0	0	61.9184	47.8576	61.5183	47.4663	61.1995	47.1531
		0.1	62.9391	47.2459	62.5822	46.8973	62.2985	46.6186
		0.3	66.0623	45.5665	65.7929	45.3038	65.5802	45.0943
	1	0	61.7044	47.4926	61.3029	47.0983	60.9830	46.7826
		0.1	62.7665	46.9207	62.4086	46.5696	62.1241	46.2889
		0.3	65.9770	45.3233	65.7073	45.0592	65.4943	44.8485
	2	0	61.6205	47.3295	61.2184	46.9338	60.8981	46.6170
		0.1	62.7038	46.7773	62.3455	46.4252	62.0607	46.1436
		0.3	65.9597	45.2203	65.6899	44.9555	65.4768	44.7444
0.1421	0	0	61.9073	47.8490	61.5071	47.4577	61.1883	47.1444
		0.1	62.9278	47.2374	62.5708	46.8887	62.2871	46.6099
		0.3	66.0504	45.5583	65.7810	45.2955	65.5683	45.0860
	1	0	61.6933	47.4839	61.2917	47.0896	60.9717	46.7738
		0.1	62.7552	46.9121	62.3972	46.5610	62.1126	46.2803
		0.3	65.9651	45.3151	65.6954	45.0509	65.4823	44.8402
	2	0	61.6093	47.3208	61.2072	46.9251	60.8868	46.6082
		0.1	62.6925	46.7687	62.3341	46.4165	62.0493	46.1349
		0.3	65.9478	45.2120	65.6780	44.9472	65.4649	44.7360

TABLE 6A. The first dimensionless frequency ($\Omega = \sqrt[4]{\rho_c A \omega^2 L^4 / E_c I}$) of porous functionally graded nanobeams under a hygro-thermal environment for C-C boundary condition ($L/h=20$).

η [nm]	ΔC	p	$\Delta T = 0$		$\Delta T = 40$ [K]		$\Delta T = 80$ [K]	
			$k = 0.5$	$k = 2$	$k = 0.5$	$k = 2$	$k = 0.5$	$k = 2$
0	0	0	15.5919	12.0512	15.3709	11.8348	15.1933	11.6596
		0.1	15.8490	11.8972	15.6519	11.7044	15.4941	11.5488
		0.3	16.6354	11.4743	16.4868	11.3292	16.3689	11.2126
	1	0	15.4740	11.8494	15.2510	11.6288	15.0719	11.4502
		0.1	15.7538	11.7174	15.5554	11.5214	15.3965	11.3631
		0.3	16.5885	11.3400	16.4394	11.1930	16.3211	11.0749
	2	0	15.4275	11.7585	15.2038	11.5360	15.0240	11.3558
		0.1	15.7192	11.6376	15.5203	11.4401	15.3610	11.2805
		0.3	16.5789	11.2828	16.4298	11.1350	16.3114	11.0162
0.1421	0	0	15.5903	12.0499	15.3692	11.8335	15.1916	11.6584
		0.1	15.8473	11.8959	15.6502	11.7032	15.4924	11.5476
		0.3	16.6337	11.4731	16.4851	11.3280	16.3672	11.2114
	1	0	15.4723	11.8481	15.2494	11.6275	15.0702	11.4489
		0.1	15.7522	11.7162	15.5538	11.5201	15.3948	11.3618
		0.3	16.5867	11.3388	16.4377	11.1918	16.3194	11.0737
	2	0	15.4259	11.7572	15.2022	11.5347	15.0224	11.3545
		0.1	15.7175	11.6364	15.5186	11.4388	15.3593	11.2792
		0.3	16.5772	11.2816	16.4280	11.1338	16.3096	11.0149

TABLE 6B. The second dimensionless frequency ($\Omega = \sqrt[4]{\rho_c A \omega^2 L^4 / E_c I}$) of porous functionally graded nanobeams under a hygro-thermal environment for C-C boundary condition ($L/h=20$).

η [nm]	ΔC	p	$\Delta T = 0$		$\Delta T = 40$ [K]		$\Delta T = 80$ [K]	
			$k = 0.5$	$k = 2$	$k = 0.5$	$k = 2$	$k = 0.5$	$k = 2$
0	0	0	42.9798	33.2197	42.6809	32.9273	42.4425	32.6930
		0.1	43.6883	32.7951	43.4217	32.5346	43.2095	32.3261
		0.3	45.8563	31.6294	45.6550	31.4331	45.4960	31.2764
	1	0	42.8200	32.9469	42.5198	32.6519	42.2805	32.4155
		0.1	43.5594	32.5521	43.2919	32.2895	43.0790	32.0793
		0.3	45.7926	31.4477	45.5910	31.2502	45.4318	31.0925
	2	0	42.7572	32.8250	42.4566	32.5288	42.2169	32.2914
		0.1	43.5126	32.4449	43.2447	32.1814	43.0316	31.9704
		0.3	45.7796	31.3707	45.5780	31.1726	45.4187	31.0145
0.1421	0	0	42.9700	33.2121	42.6710	32.9197	42.4326	32.6853
		0.1	43.6783	32.7876	43.4116	32.5270	43.1995	32.3185
		0.3	45.8457	31.6221	45.6445	31.4258	45.4855	31.2691
	1	0	42.8101	32.9393	42.5099	32.6443	42.2705	32.4078
		0.1	43.5494	32.5445	43.2818	32.2819	43.0690	32.0717
		0.3	45.7820	31.4404	45.5805	31.2429	45.4212	31.0852
	2	0	42.7474	32.8173	42.4467	32.5211	42.2069	32.2836
		0.1	43.5025	32.4373	43.2347	32.1738	43.0216	31.9628
		0.3	45.7691	31.3634	45.5675	31.1653	45.4082	31.0072

TABLE 6C. The third dimensionless frequency ($\Omega = \sqrt[4]{\rho_c A \omega^2 L^4 / E_c I}$) of porous functionally graded nanobeams under a hygro-thermal environment for C-C boundary condition ($L/h=20$).

η [nm]	ΔC	p	$\Delta T = 0$		$\Delta T = 40$ [K]		$\Delta T = 80$ [K]	
			$k = 0.5$	$k = 2$	$k = 0.5$	$k = 2$	$k = 0.5$	$k = 2$
0	0	0	84.2592	65.1250	83.9322	64.8054	83.6723	64.5503
		0.1	85.6481	64.2926	85.3565	64.0078	85.1250	63.7807
		0.3	89.8982	62.0074	89.6780	61.7926	89.5043	61.6217
	1	0	84.0842	64.8268	83.7566	64.5057	83.4961	64.2494
		0.1	85.5070	64.0269	85.2148	63.7409	84.9830	63.5128
		0.3	89.8284	61.8086	89.6080	61.5931	89.4343	61.4217
	2	0	84.0156	64.6939	83.6877	64.3721	83.4270	64.1152
		0.1	85.4557	63.9100	85.1634	63.6234	84.9314	63.3949
		0.3	89.8143	61.7245	89.5938	61.5087	89.4200	61.3371
0.1421	0	0	84.2256	65.0991	83.8986	64.7794	83.6386	64.5242
		0.1	85.6140	64.2670	85.3222	63.9821	85.0908	63.7550
		0.3	89.8624	61.9826	89.6421	61.7678	89.6484	61.5969
	1	0	84.0506	64.8008	83.7229	64.4796	83.4624	64.2232
		0.1	85.4728	64.0012	85.1806	63.7151	84.9487	63.4870
		0.3	89.7926	61.7838	89.5721	61.5683	89.3983	61.3969
	2	0	83.9820	64.6678	83.6540	64.3460	83.3933	64.0890
		0.1	85.4216	63.8843	85.1291	63.5977	84.8971	63.3691
		0.3	89.7784	61.6997	89.5579	61.4839	89.3841	61.3122

TABLE 7A. The first dimensionless frequency ($\Omega = \sqrt[4]{\rho_c A \omega^2 L^4 / E_c I}$) of porous functionally graded nanobeams under a hygro-thermal environment for C-S boundary condition ($L/h=20$).

η [nm]	ΔC	p	$\Delta T = 0$		$\Delta T = 40$ [K]		$\Delta T = 80$ [K]	
			$k = 0.5$	$k = 2$	$k = 0.5$	$k = 2$	$k = 0.5$	$k = 2$
0	0	0	10.7447	8.3047	10.4423	8.0081	10.1960	7.7637
		0.1	10.9218	8.1986	10.6525	7.9346	10.4342	7.7181
		0.3	11.4638	7.9072	11.2611	7.7088	11.0989	7.5475
	1	0	10.5839	8.0282	10.2764	7.7202	10.0257	7.4657
		0.1	10.7923	7.9526	10.5194	7.6796	10.2980	7.4552
		0.3	11.4000	7.7237	11.1960	7.5202	11.0328	7.3545
	2	0	10.5202	7.9021	10.2107	7.5885	9.9582	7.3366
		0.1	10.7449	7.8421	10.4707	7.5648	10.2482	7.3292
		0.3	11.3870	7.6449	11.1828	7.4391	11.0193	7.2714
0.1421	0	0	10.7441	8.3042	10.4417	8.0076	10.1953	7.7632
		0.1	10.9212	8.1981	10.6519	7.9342	10.4335	7.7177
		0.3	11.4631	7.9067	11.2604	7.7084	11.0982	7.5471
	1	0	10.5833	8.0278	10.2758	7.7197	10.0251	7.4652
		0.1	10.7916	7.9521	10.5187	7.6791	10.2974	7.4547
		0.3	11.3993	7.7233	11.1954	7.5198	11.0321	7.3540
	2	0	10.5196	7.9016	10.2101	7.5880	9.9576	7.3361
		0.1	10.7443	7.8416	10.4700	7.5643	10.2476	7.3287
		0.3	11.3863	7.6444	11.1821	7.4386	11.0186	7.2709

TABLE 7B. The second dimensionless frequency ($\Omega = \sqrt[4]{\rho_c A \omega^2 L^4 / E_c I}$) of porous functionally graded nanobeams under a hygro-thermal environment for C-S boundary condition ($L/h=20$).

η [nm]	ΔC	p	$\Delta T = 0$		$\Delta T = 40$ [K]		$\Delta T = 80$ [K]	
			$k = 0.5$	$k = 2$	$k = 0.5$	$k = 2$	$k = 0.5$	$k = 2$
0	0	0	34.8198	26.9127	34.4757	26.5760	34.2006	26.3053
		0.1	35.3938	26.5687	35.0869	26.2688	34.8422	26.0281
		0.3	37.1502	25.6244	36.9186	25.3984	36.7354	25.2177
	1	0	34.6359	26.5986	34.2899	26.2578	34.0133	25.9838
		0.1	35.2455	26.2889	34.9372	25.9857	34.6914	25.7423
		0.3	37.0769	25.4152	36.8449	25.1873	36.6613	25.0051
	2	0	34.5637	26.4579	34.2169	26.1152	33.9397	25.8397
		0.1	35.1916	26.1653	34.8828	25.8606	34.6367	25.6160
		0.3	37.0620	25.3264	36.8299	25.0977	36.6462	24.9148
0.1421	0	0	34.8146	26.9087	34.4704	26.5719	34.1953	26.3012
		0.1	35.3885	26.5647	35.0815	26.2648	34.8368	26.0240
		0.3	37.1446	25.6205	36.9130	25.3945	36.7297	25.2138
	1	0	34.6307	26.5946	34.2846	26.2537	34.0079	25.9797
		0.1	35.2402	26.2849	34.9319	25.9817	34.6861	25.7383
		0.3	37.0713	25.4114	36.8393	25.1834	36.6557	25.0012
	2	0	34.5584	26.4538	34.2116	26.1111	33.9343	25.8355
		0.1	35.1862	26.1612	34.8774	25.8565	34.6313	25.6119
		0.3	37.0564	25.3225	36.8243	25.0938	36.6406	24.9109

TABLE 7C. The third dimensionless frequency ($\Omega = \sqrt[4]{\rho_c A \omega^2 L^4 / E_c I}$) of porous functionally graded nanobeams under a hygro-thermal environment for C-S boundary condition ($L/h=20$).

η [nm]	ΔC	p	$\Delta T = 0$		$\Delta T = 40$ [K]		$\Delta T = 80$ [K]	
			$k = 0.5$	$k = 2$	$k = 0.5$	$k = 2$	$k = 0.5$	$k = 2$
0	0	0	72.6498	56.1520	72.2891	55.7993	72.0021	55.5175
		0.1	73.8474	55.4343	73.5256	55.1200	73.2701	54.8692
		0.3	77.5119	53.4639	77.2690	53.2270	77.0773	53.0383
	1	0	72.4568	55.8230	72.0951	55.4682	71.8074	55.1847
		0.1	73.6917	55.1411	73.3692	54.8252	73.1132	54.5730
		0.3	77.4350	53.2446	77.1918	53.0067	76.9999	52.8173
	2	0	72.3811	55.6762	72.0191	55.3205	71.7310	55.0362
		0.1	73.6352	55.0120	73.3125	54.6953	73.0562	54.4425
		0.3	77.4193	53.1518	77.1761	52.9135	76.9842	52.7237
0.1421	0	0	72.6290	56.1359	72.2682	55.7832	71.9811	55.5013
		0.1	73.8262	55.4184	73.5044	55.1041	73.2488	54.8532
		0.3	77.4896	53.4485	77.2467	53.2116	77.0550	53.0229
	1	0	72.4359	55.8068	72.0742	55.4520	71.7864	55.1684
		0.1	73.6705	55.1251	73.3479	54.8092	73.0918	54.5569
		0.3	77.4127	53.2292	77.1695	52.9913	76.9776	52.8018
	2	0	72.3603	55.6600	71.9981	55.3042	71.7100	55.0198
		0.1	73.6140	54.9960	73.2912	54.6793	73.0349	54.4264
		0.3	77.3971	53.1364	77.1538	52.8980	76.9619	52.7082

because the FG nanobeam becomes stiffer for higher values of the power-law index; when the increase of volume fraction of metal causes the reduction in the value of Young's modulus of the FG beam. It is interesting to underline that the dimensionless natural frequencies increase or decrease with the volume fraction of porosity (p) depending on the values of the material gradation index (k). The dimensionless frequencies increase with increasing the porosity volume fraction at $k = 0.5$ whereas they decrease with increasing the porosity ratio at $k = 2$. It means that the material composition plays a significant role on the free vibration behaviour of porous FG nanobeam models. Moreover, in the case of $k = 0.5$, the variations of the dimensionless natural frequencies with the porosity ratio are faster than when $k = 2$. The natural frequencies become more sensitive to the variations of the porosity ratio when $k = 0.5$.

For further investigating the impacts of the temperature rise and porosity ratio on the vibration behaviours of the FG nanobeam, Fig. 4 demonstrates the variation of the first and third modes of vibration frequencies with the porosity index (p) at the constant slenderness ratio ($L/h = 20$), the power-law index ($k = 1$) and the moisture concentration ($\Delta C = 2$). It is seen that for all boundary conditions, dimensionless frequencies linearly increase with increasing the porosity ratio for both classical elasticity and DM models. These results are different from some of those results are given in Tables 5–7 because of the difference in the material grading index, where k is 2 in the previous comparison. The DM model always predicts lower values than classical elasticity results and this phenomenon is more apparent especially for higher modes of vibration ($n = 3$). However, the difference between two theories is very small for the first mode of vibration ($n = 1$). This is due to the small-scale effects are insignificant at lower modes of vibration. Also, it is seen that dimensionless frequencies decrease by increasing the temperature change (both classical elasticity and DM) and it can be stated that the linear temperature change is a key factor in the free vibration behaviour of porous FG nanobeams.

In Fig. 5, the effects of the porosity ratio and the moisture concentration on the first and third dimensionless frequencies of S-S, C-C and C-S FG nanobeam have been shown. Here, the temperature rise of the hygro-thermal environment is set to be 40 K. It can be observed that the changes of the moisture concentrations have considerable effects on the free vibration of the FG nanobeams with porosity. The dimensionless frequencies decrease with increasing the moisture concentrations for all given boundary conditions. It is also notable that the vibration frequencies become more sensitive to the variations of the porosity ratio, especially for higher moisture concentrations ($\Delta C = 10$). This result provides that the rise of moisture concentration makes the beam buckled at the considered hygro-thermal environments with a linear temperature rise and the increase of the moisture leads to the reduction in the rigidity of the beam.

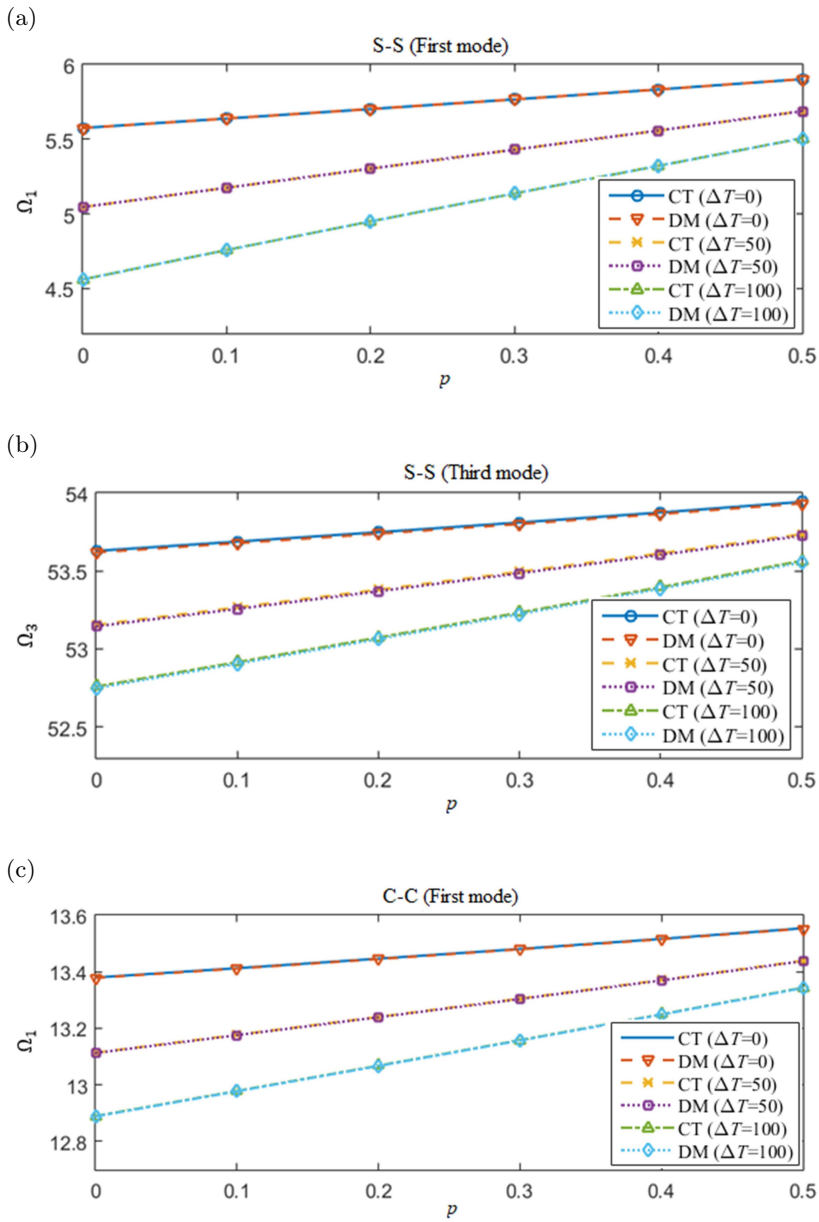


FIG. 4. Effect of p and ΔT on the first and third vibration frequencies ($L/h = 20$, $k = 1$, $\Delta C = 2$, $\eta = 0.1421$ nm).

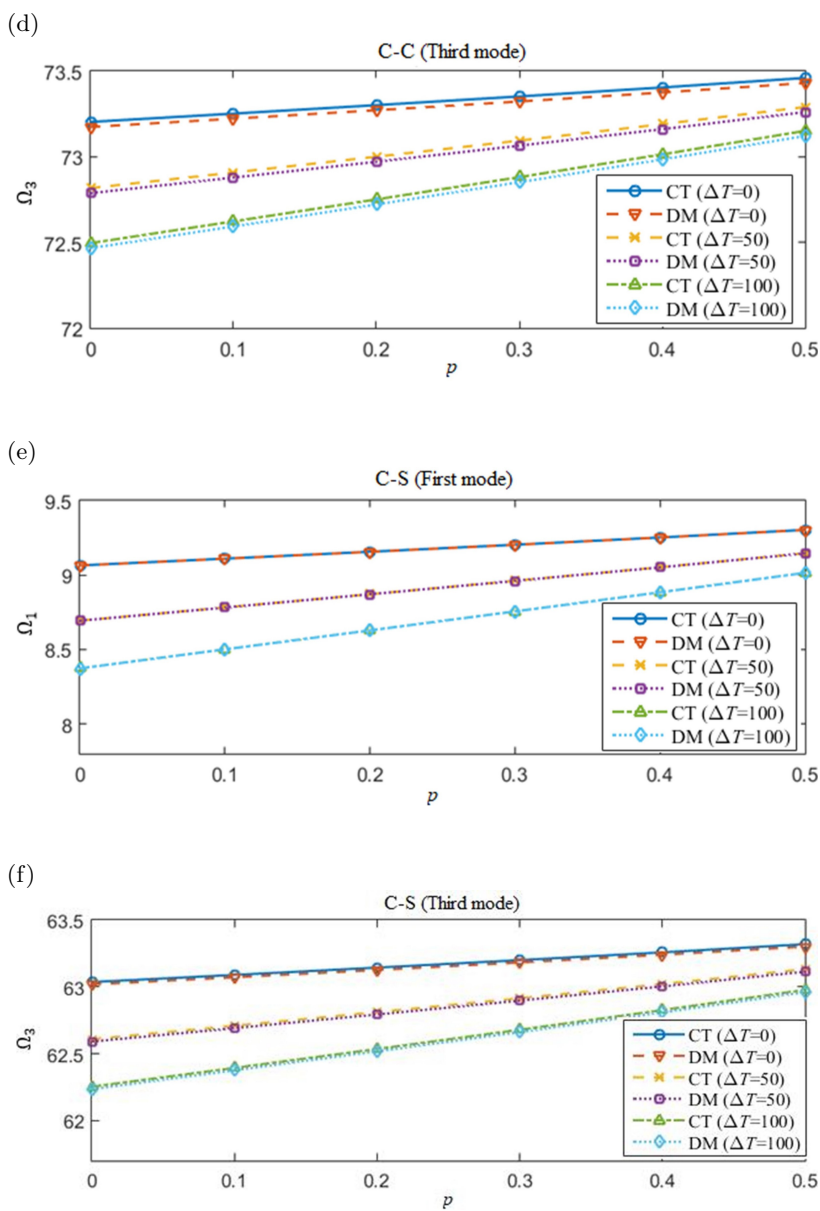


FIG 4. [cont.]

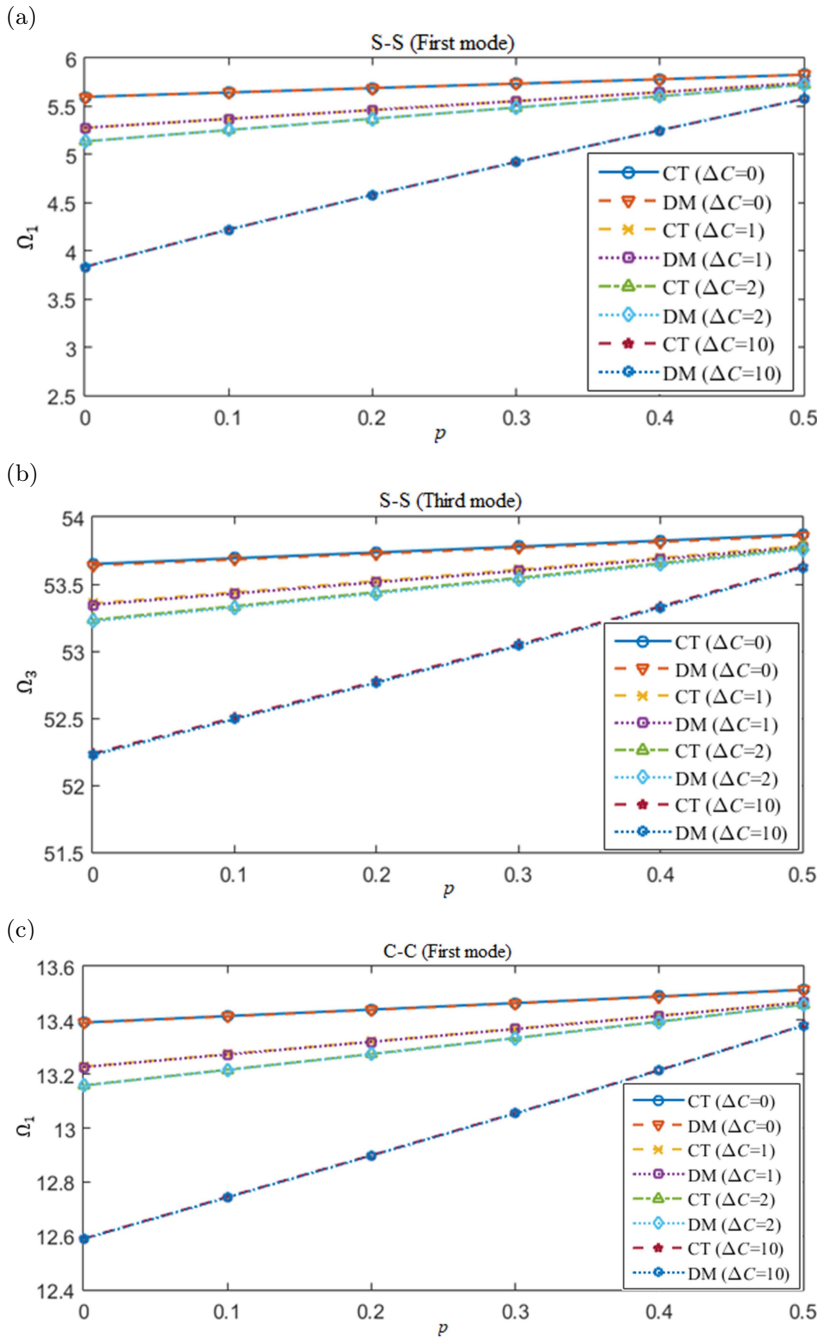


FIG. 5. Effect of p and ΔC on the first and third vibration frequencies ($L/h = 20, k = 1, \Delta T = 40, \eta = 0.1421 \text{ nm}$).

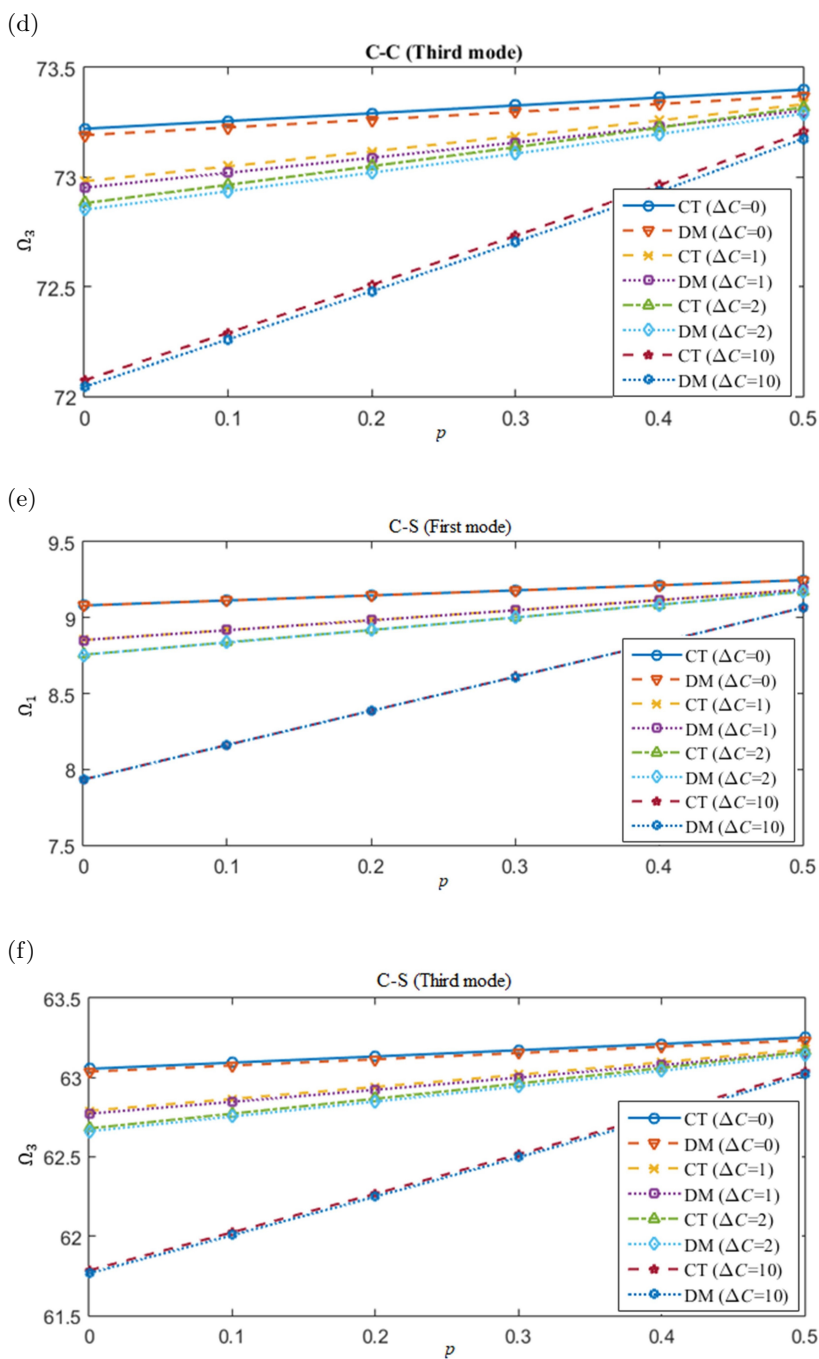


FIG 5. [cont.]

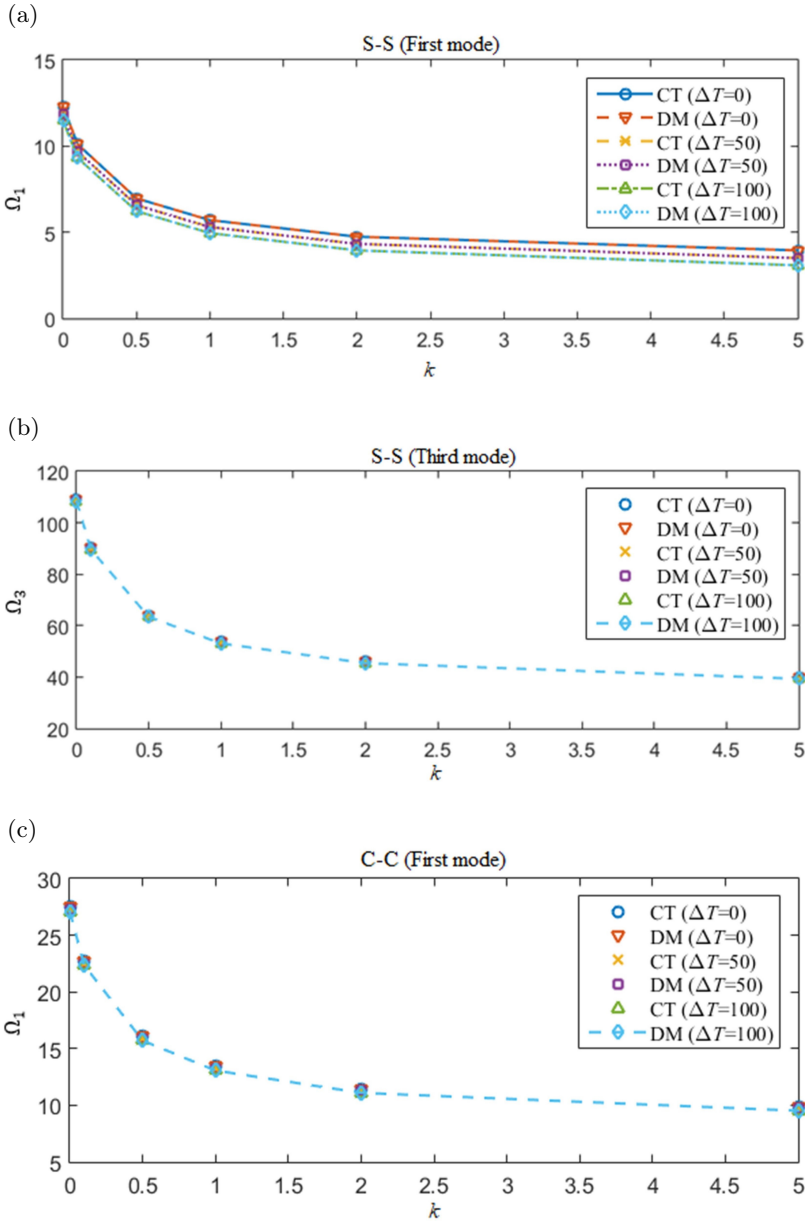


FIG. 6. Effect of k and ΔT on the first and third vibration frequencies ($L/h = 20$, $p = 0.2$, $\Delta C = 2$, $\eta = 0.1421$ nm).

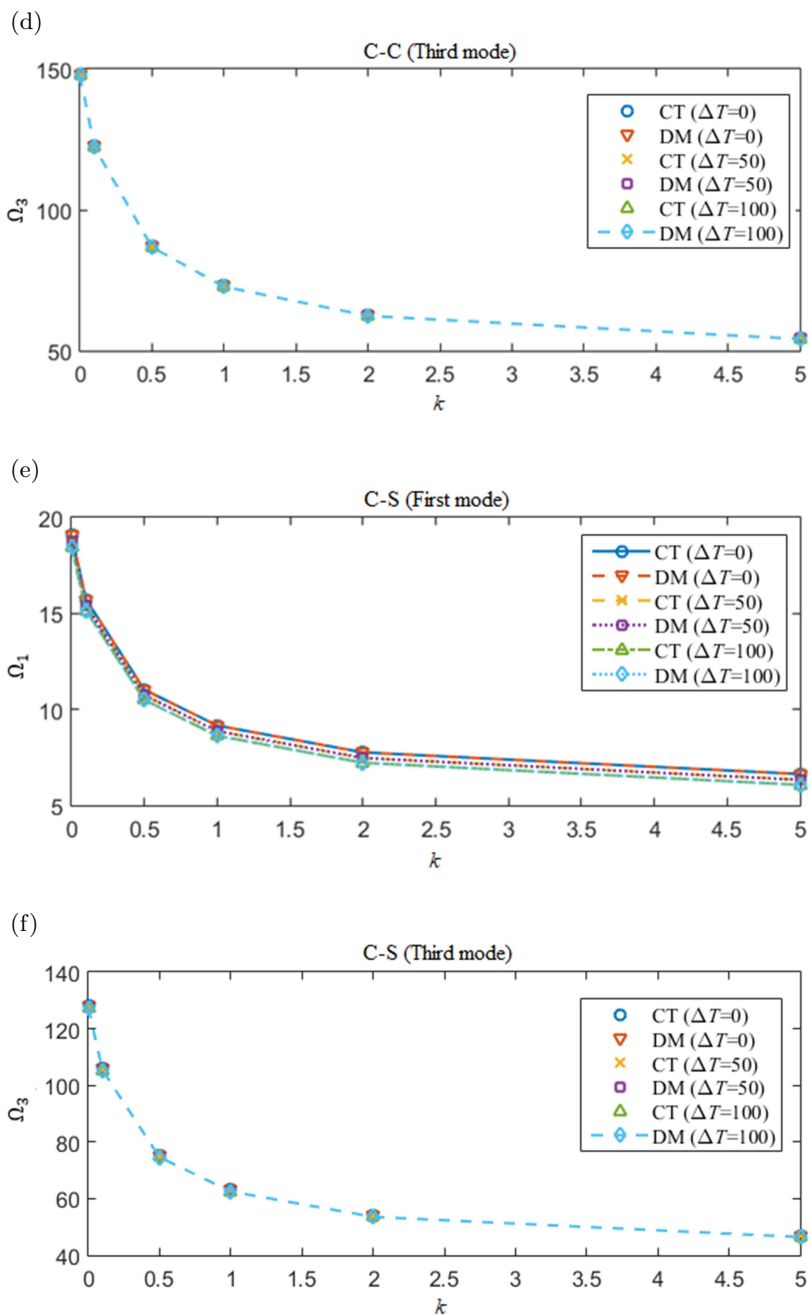


FIG 6. [cont.]

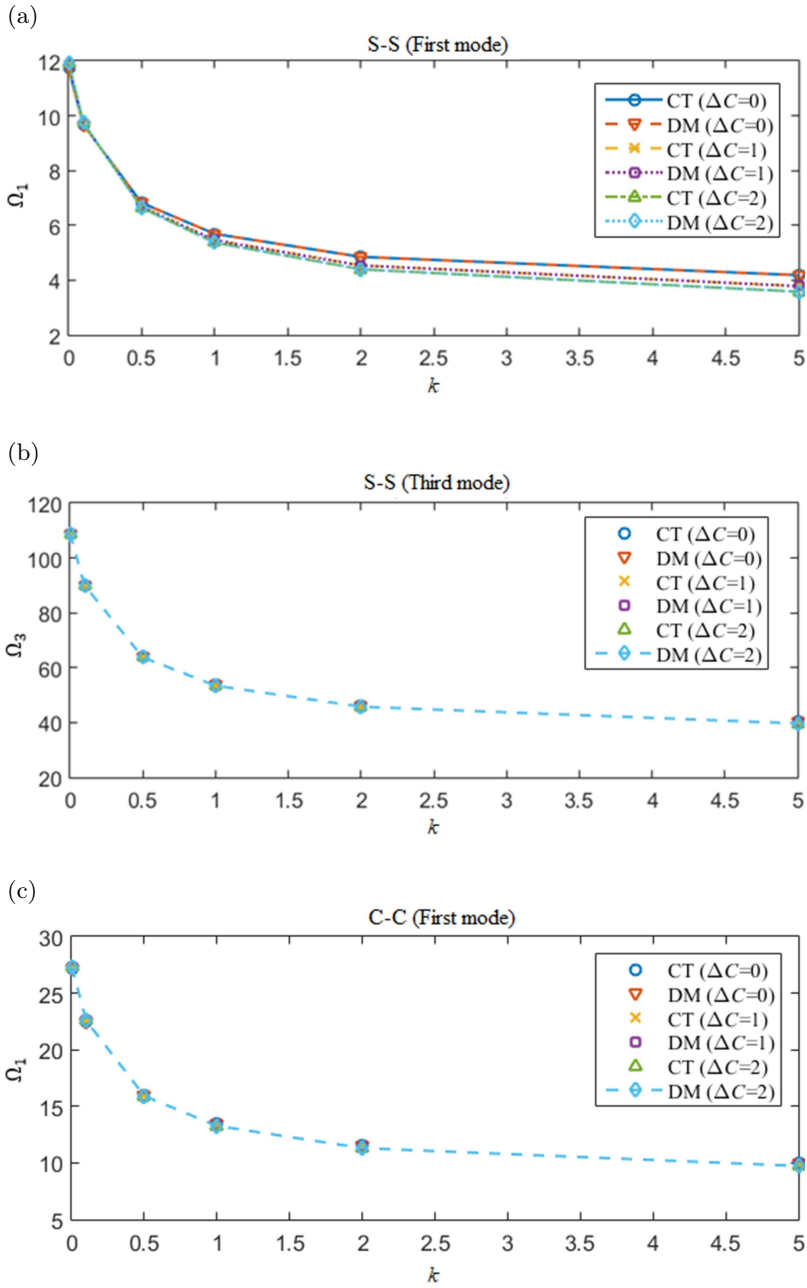


FIG. 7. Effect of k and ΔC on the first and third vibration frequencies ($L/h = 20$, $p = 0.2$, $\Delta T = 40$, $\eta = 0.1421$ nm).

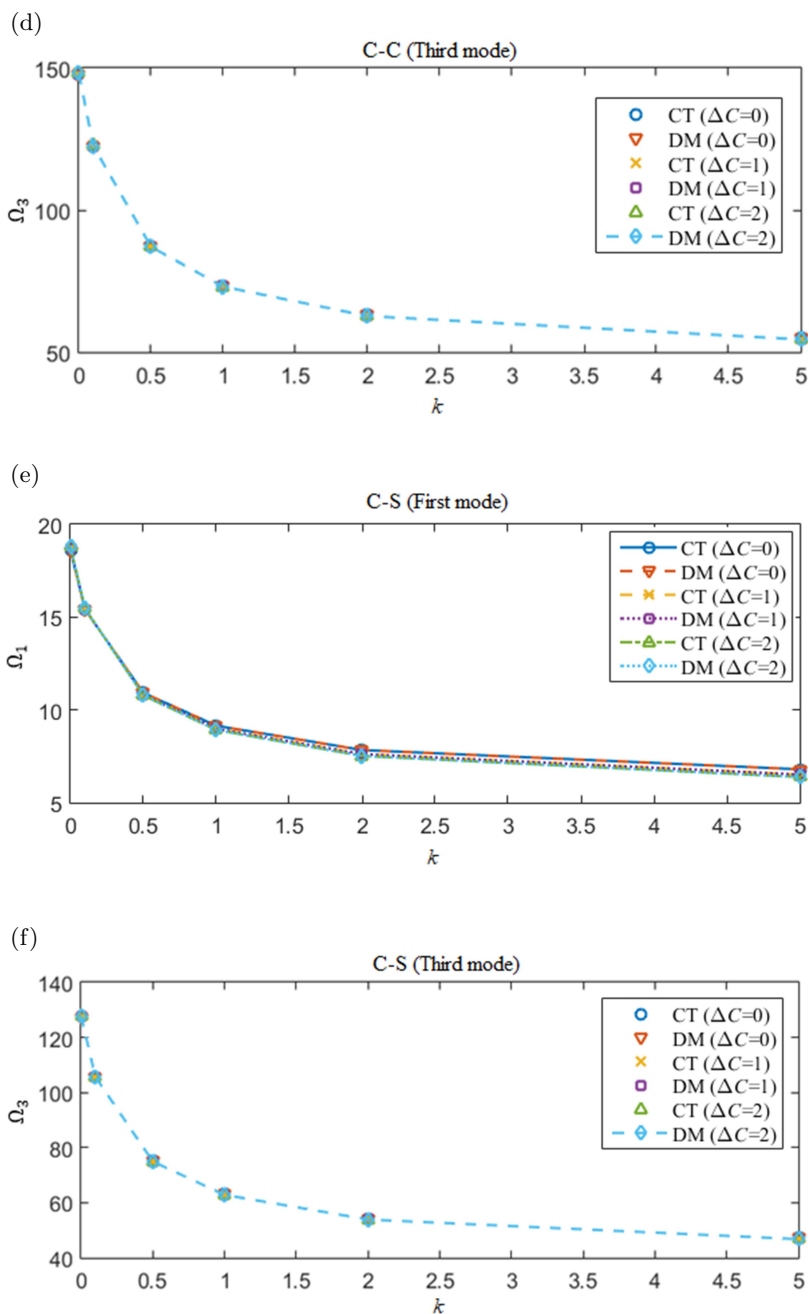


FIG 7. [cont.]

As it is similar to Fig. 4, the dimensionless frequencies increase with increasing the porosity ratio for both classical and DM models. A softening structural response has been exhibited by the DM formulation for all boundary conditions.

Figure 6 demonstrates the variation of the first and third dimensionless frequencies with changing of the temperature rise at the constant porosity ratio ($p = 0.2$), the slenderness ratio ($L/h = 20$) and the moisture concentration ($\Delta C = 2$) of the FG nanobeam with the different power-law index and different boundary conditions. The frequency results obtained from the classical elasticity theory ($\eta = 0$) is always the greatest one. There is a nonlinear decrease for the first and third dimensionless frequencies as the power-law index increase, and this decrease is more important when the values of k are less than 2. After $k > 2$, the decrease in the natural frequencies slows till it gets limits for higher k values, at which the composition of material is liable to pure metal. The dimensionless frequencies decrease as the temperature rises. This reduction in natural frequency is due to the thermally induced compressive stress weakens the stiffness of the FG nanobeam. As it is expected, the FG nanobeam under the hygro-thermal environment gives higher natural frequencies at stiffer beam edges (C-C and C-S).

The influences of material gradation and moisture concentration on the first and third dimensionless frequencies of the porous FG nanobeam have been shown in Fig. 7. The increasing the power-law index and moisture concentrations yields the reduction in dimensionless frequencies for all given boundary conditions, which highlights the importance of the moisture and material gradation effects.

Figure 8 shows the variation of the fundamental frequency (first dimensionless frequency) with different values of linear temperature changes for based on the DM model. The fundamental frequencies of the FG nanobeam under the hygro-thermal environment decrease with increasing the temperature difference until it converges to the critical buckling temperature. The fundamental frequencies of the FG nanobeam decreases with the rise of temperature until it reaches zero at the critical temperature point. This is due to the decrease in the stiffness of the beam when temperature increases. It is also notable that the fundamental frequencies have dropped sharply and approached to zero value when the temperature difference converges to a certain value. Similar to previous results, the porosity increases the fundamental frequencies for all boundary conditions.

In Fig. 9, the impacts of the moisture concentration and the porosity ratio on the free vibration of FG nanobeams are presented for both classical elasticity and DM theories. It can be seen that the first and third dimensionless frequencies decrease with increasing the moisture concentration for both classical and DM theories. Moreover, dimensionless frequencies increase with increasing the porosity ratio for the given power-law index ($k = 1$). It is worthy to note that

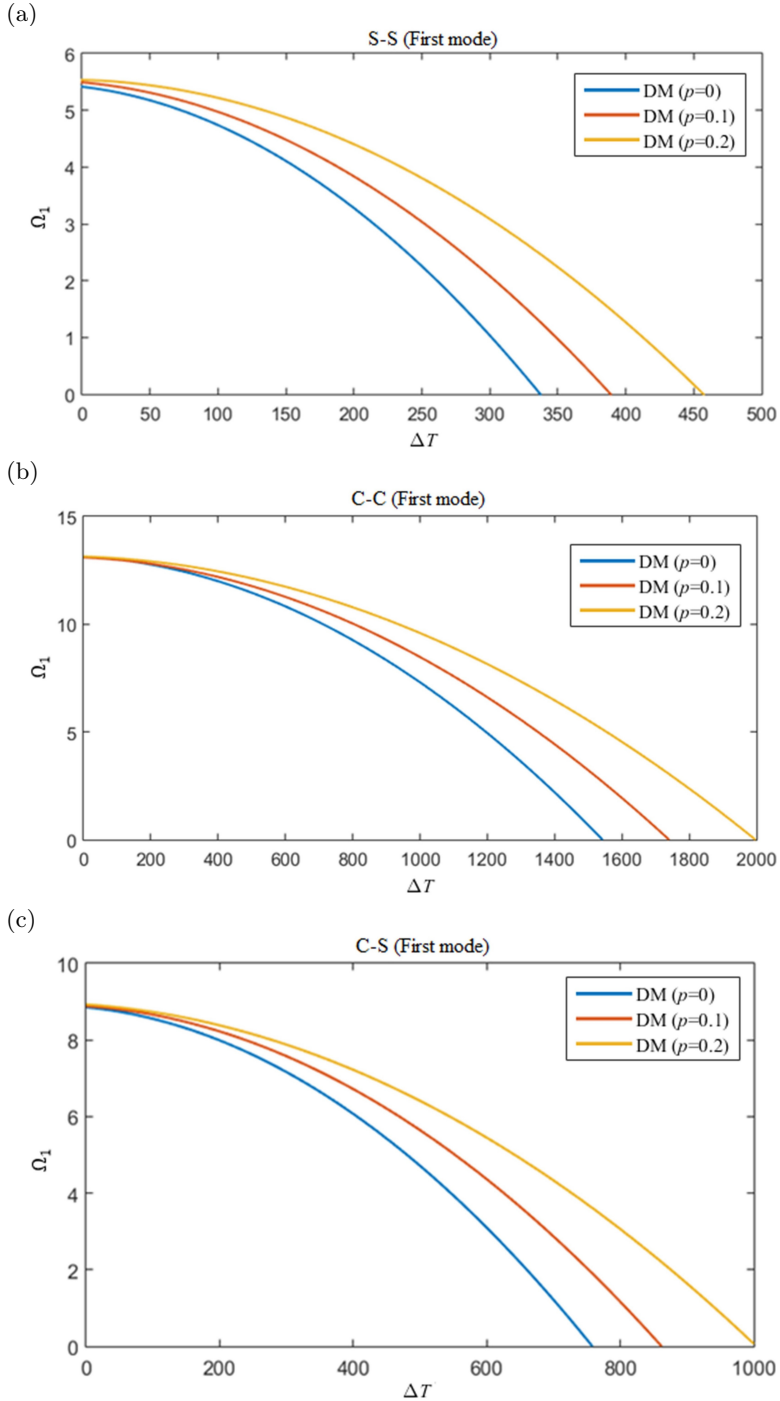


FIG. 8. Effect of temperature change ΔT on the first vibration frequency for different values of porosity ratios ($L/h = 20$, $k = 1$, $\Delta C = 2$, $\eta = 0.1421$ nm).

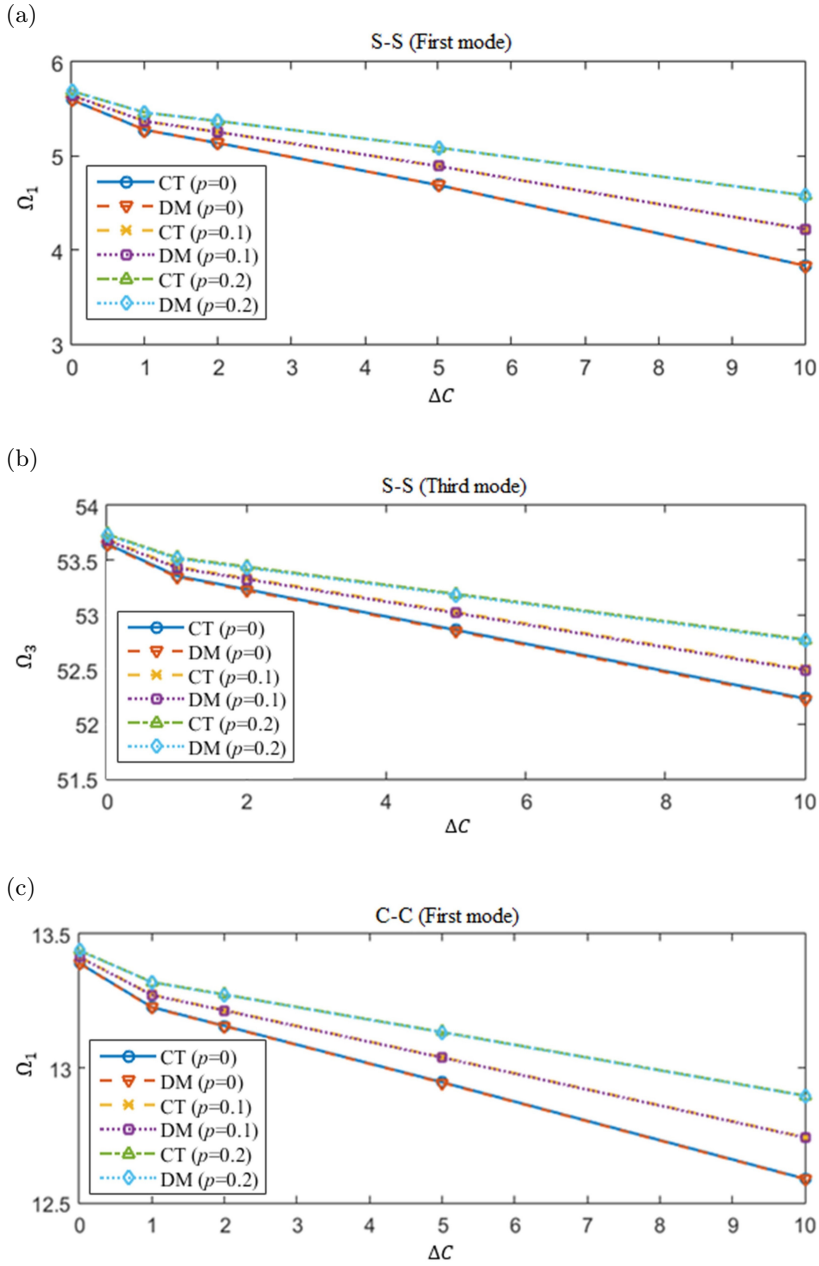


FIG. 9. Effect of ΔC and p on the first and third vibration frequencies ($L/h = 20$, $k = 1$, $\Delta T = 40$, $\eta = 0.1421$ nm).

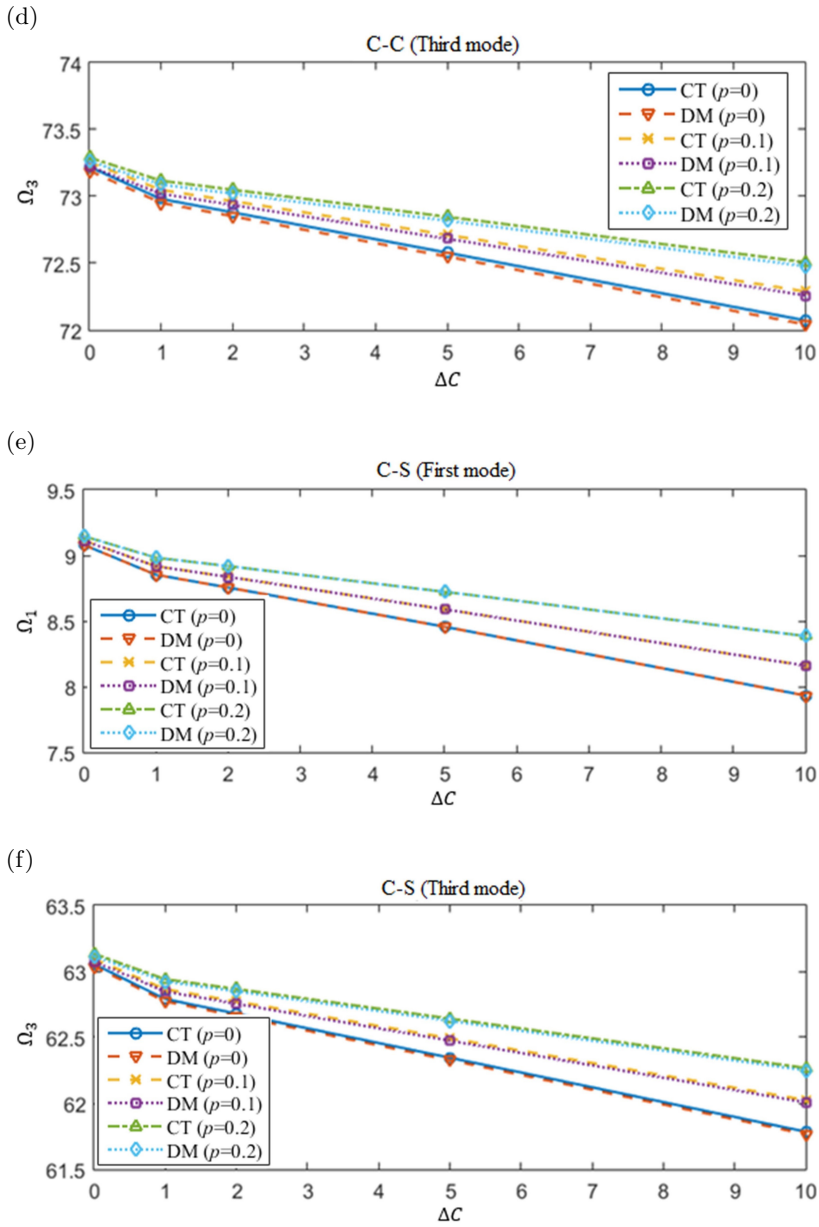


FIG 9. [cont.]

the dimensionless frequencies become more sensitive to the variations of moisture environments, while the moisture concentration converges to a certain value. This phenomenon shows that the moisture plays a significant role in the vibration behaviour of porous FG nanobeams.

7. Conclusions

Hygro-thermal vibration behaviour of the FG porous nanobeams with various boundary conditions is examined based on the size-dependent DM theory in conjunction with the Ritz method. Hygro-thermo-mechanical properties of the FG nanobeams are assumed to be functions of the thickness, temperature and porosity. The formulation of the Euler–Bernoulli beam theory is used to model the FG nanobeam. The influences of linear temperature rise, moisture concentration, porosity volume fraction, material grading index and material length scale parameter on the free vibration response of the FG nanobeam are investigated in detail. From the present study, we can draw the following remarkable conclusions:

- The hygro-thermal environments play a significant role on the free vibration behaviour of FG porous nanobeams. The increase of the temperature and moisture concentrations decreases the natural frequencies. This decrease in natural frequency is due to the thermally induced compressive stress and rise in moisture concentration, which reduce the rigidity of the FG nanobeam.

- The natural frequencies increase or decrease with the volume fraction of porosity depending on the values of the material grading index. The increase occurs in dimensionless frequencies of the nanobeam with increasing the porosity volume fraction when material graduation index equals to $k = 0.5$, whereas the trend is reverse at $k = 2$. It means that the material composition changes the free vibration behaviour of porous FG nanobeam models.

- The natural frequencies become more sensitive to the variations of the porosity ratio, especially for higher moisture concentrations.

- Increasing the power-law index, the natural frequencies decreases. Since, the amount of the ceramic constituent in the FG nanobeam increases when the material grading index approaches to zero and this causes the increase of the natural frequencies. However, the increase of the material grading index causes the increase of the metal constituent in the FG nanobeam and natural frequencies decrease.

- The softening material response is predicted by the size-dependent DM theory compared to the classical elasticity theory for all given boundary conditions. The difference between two theories is more apparent for higher modes of vibration.

References

1. Y. HUI, J.S. GOMEZ-DIAZ, Z. QIAN, A. ALU, M. RINALDI, *Plasmonic piezoelectric nanomechanical resonator for spectrally selective infrared sensing*, Nature Communications, **7**, 1, 11249, 2016.
2. M. SOLTAN REZAEE, M. AFRASHI, *Modeling the nonlinear pull-in behavior of tunable nano-switches*, International Journal of Engineering Science, **109**, 73–87, 2016.
3. S. RAHMANIAN, S. HOSSEINI-HASHEMI, *Size-dependent resonant response of a double-layered viscoelastic nanoresonator under electrostatic and piezoelectric actuations incorporating surface effects and Casimir regime*, International Journal of Non-Linear Mechanics, **109**, 118–131, 2019.
4. R. BASUTKAR, *Analytical modelling of a nanoscale series-connected bimorph piezoelectric energy harvester incorporating the flexoelectric effect*, International Journal of Engineering Science, **139**, 42–61, 2019.
5. M. RAHAEIFARD, M.H. KAHROBAIYAN, M.T. AHMADIAN, *Sensitivity analysis of atomic force microscope cantilever made of functionally graded materials*, International Design Engineering Technical Conferences and Computers and Information in Engineering Conference, **49033**, 539–544, 2009.
6. Y. MOSER, M.A. GIJS, *Miniaturized flexible temperature sensor*, Journal of Microelectromechanical Systems, **16**, 6, 1349–1354, 2007.
7. Q. WANG, *Wave propagation in carbon nanotubes via nonlocal continuum mechanics*, Journal of Applied Physics, **98**, 12, 124301, 2005.
8. Q. WANG, V.K. VARADAN, *Vibration of carbon nanotubes studied using nonlocal continuum mechanics*, Smart Materials and Structures, **15**, 2, 659, 2006.
9. R. TOUPIN, *Elastic materials with couple-stresses*, Archive for Rational Mechanics and Analysis, **11**, 1, 385–414, 1962.
10. A.C. ERINGEN, *On differential equations of nonlocal elasticity and solutions of screw dislocation and surface waves*, Journal of Applied Physics, **54**, 9, 4703–4710, 1983.
11. R.D. MINDLIN, *Micro-structure in linear elasticity*, Archive for Rational Mechanics and Analysis, **16**, 51–78, 1964.
12. C.W. LIM, G. ZHANG, J.N. REDDY, *A higher-order nonlocal elasticity and strain gradient theory and its applications in wave propagation*, Journal of the Mechanics and Physics of Solids, **78**, 298–313, 2015.
13. S.A. SILLING, *Reformulation of elasticity theory for discontinuities and long-range forces*, Journal of the Mechanics and Physics of Solids, **48**, 1, 175–209, 2000.
14. F.A.C.M. YANG, A.C.M. CHONG, D.C.C. LAM, P. TONG, *Couple stress based strain gradient theory for elasticity*, International Journal of Solids and Structures, **39**, 10, 2731–2743, 2002.
15. G. ROMANO, R. BARRETTA, *Nonlocal elasticity in nanobeams: the stress-driven integral model*, International Journal of Engineering Science, **115**, 14–27, 2017.
16. V.T. GRANIK, *Microstructural mechanics of granular media*, Technique Report IM/MGU, Institute of Mechanics of Moscow State University, pp. 78–241, 1978.
17. L.L. KE, Y.S. WANG, *Size effect on dynamic stability of functionally graded microbeams based on a modified couple stress theory*, Composite Structures, **93**, 2, 342–350, 2011.
18. J.N. REDDY, *Microstructure-dependent couple stress theories of functionally graded beams*, Journal of the Mechanics and Physics of Solids, **59**, 11, 2382–2399, 2011.

19. M. ŞİMŞEK, J.N. REDDY, *Bending and vibration of functionally graded microbeams using a new higher order beam theory and the modified couple stress theory*, International Journal of Engineering Science, **64**, 37–53, 2013.
20. B. AKGÖZ, Ö. CİVALEK, *Buckling analysis of functionally graded microbeams based on the strain gradient theory*, Acta Mechanica, **224**, 9, 2185–2201, 2013.
21. B. AKGÖZ, Ö. CİVALEK, *Shear deformation beam models for functionally graded microbeams with new shear correction factors*, Composite Structures, **112**, 214–225, 2014.
22. O. RAHMANI, O. PEDRAM, *Analysis and modeling the size effect on vibration of functionally graded nanobeams based on nonlocal Timoshenko beam theory*, International Journal of Engineering Science, **77**, 55–70, 2014.
23. U. GUL, M. AYDOĞDU, *Dynamic analysis of functionally graded beams with periodic nanostructures*, Composite Structures, **257**, 113169, 2021.
24. U. GUL, M. AYDOĞDU, *Buckling analysis of functionally graded beams with periodic nanostructures using doublet mechanics theory*, Journal of the Brazilian Society of Mechanical Sciences and Engineering, **43**, 1–8, 2021.
25. L. LI, Y. HU, *Nonlinear bending and free vibration analyses of nonlocal strain gradient beams made of functionally graded material*, International Journal of Engineering Science, **107**, 77–97, 2016.
26. E.E. GHANDOURAH, H.M. AHMED, M.A. ELTAHER, M.A. ATTIA, A.M. ABDRABOH, *Free vibration of porous FG nonlocal modified couple nanobeams via a modified porosity model*, Advances in Nano Research, **11**, 4, 405–422, 2021.
27. A. MESSAI, L. FORTAS, T. MERZOUKI, M.S.A. HOUARI, *Vibration analysis of FG reinforced porous nanobeams using two variables trigonometric shear deformation theory*, Structural Engineering and Mechanics, **81**, 4, 461–479, 2022.
28. B. UZUN, M.Ö. YAYLI, *Rotary inertia effect on dynamic analysis of embedded FG porous nanobeams under deformable boundary conditions with the effect of neutral axis*, Journal of the Brazilian Society of Mechanical Sciences and Engineering, **46**, 111, 2024.
29. M. ELLALI, M. BOUAZZA, A.M. ZENKOUR, N. BENSEDDIQ, *Polynomial-exponential integral shear deformable theory for static stability and dynamic behaviors of FG-CNT nanobeams*, Archive of Applied Mechanics, **94**, 1455–1474, 2024.
30. F. EBRAHIMI, E. SALARI, *Nonlocal thermo-mechanical vibration analysis of functionally graded nanobeams in thermal environment*, Acta Astronautica, **113**, 29–50, 2015.
31. F. EBRAHIMI, E. SALARI, *Thermal buckling and free vibration analysis of size dependent Timoshenko FG nanobeams in thermal environments*, Composite Structures, **128**, 363–380, 2015.
32. F. EBRAHIMI, E. SALARI, *Thermo-mechanical vibration analysis of nonlocal temperature-dependent FG nanobeams with various boundary conditions*, Composites Part B: Engineering, **78**, 272–290, 2015.
33. F. EBRAHIMI, F. GHASEMI, E. SALARI, *Investigating thermal effects on vibration behavior of temperature-dependent compositionally graded Euler beams with porosities*, Meccanica, **51**, 223–249, 2016.
34. F.Z. JOUNEGHANI, R. DIMITRI, F. TORNABENE, *Structural response of porous FG nanobeams under hygro-thermo-mechanical loadings*, Composites Part B: Engineering, **152**, 71–78, 2018.

35. M.H. JALAEI, A.G. ARANI, H. NGUYEN-XUAN, *Investigation of thermal and magnetic field effects on the dynamic instability of FG Timoshenko nanobeam employing nonlocal strain gradient theory*, International Journal of Mechanical Sciences, **161**, 105043, 2019.
36. F. EBRAHIMI, M.R. BARATI, *A unified formulation for dynamic analysis of nonlocal heterogeneous nanobeams in hygro-thermal environment*, Applied Physics A, **122**, 1–14, 2016.
37. Y. WANG, H. REN, T. FU, C. SHI, *Hygrothermal mechanical behaviors of axially functionally graded microbeams using a refined first order shear deformation theory*, Acta Astronautica, **166**, 306–316, 2020.
38. R. PENNA, L. FEO, G. LOVISI, F. FABBROCINO, *Hygro-thermal vibrations of porous FG nano-beams based on local/nonlocal stress gradient theory of elasticity*, Nanomaterials, **11**, 4, 910, 2021.
39. R. PENNA, L. FEO, G. LOVISI, *Hygro-thermal bending behavior of porous FG nano-beams via local/nonlocal strain and stress gradient theories of elasticity*, Composite Structures, **263**, 113627, 2021.
40. Y.S. LI, B.L. LIU, J.J. ZHANG, *Hygro-thermal buckling of porous FG nanobeams considering surface effects*, Structural Engineering and Mechanics, **79**, 3, 359–371, 2021.
41. R. ÖZMEN, R. KILIÇ, I. ESEN, *Thermomechanical vibration and buckling response of nonlocal strain gradient porous FG nanobeams subjected to magnetic and thermal fields*, Mechanics of Advanced Materials and Structures, **31**, 4, 834–853, 2024.
42. F. EBRAHIMI, M. KARIMIASL, V. MAHESH, *Vibration analysis of magneto-flexo-electrically actuated porous rotary nanobeams considering thermal effects via nonlocal strain gradient elasticity theory*, Advances in Nano Research, **7**, 4, 223–231, 2019.
43. M. BENDAIDA, A.A. BOUSAHLA, A. MOUFFOKI, H. HEIRECHE, F. BOURADA, A. TOUNSI, M. HUSSAIN, *Dynamic properties of nonlocal temperature-dependent FG nanobeams under various thermal environments*, Transport in Porous Media, **142**, 1, 187–208, 2022.
44. F. EBRAHIMI, M.R. BARATI, *Vibration analysis of smart piezoelectrically actuated nanobeams subjected to magneto-electrical field in thermal environment*, Journal of Vibration and Control, **24**, 3, 549–564, 2018.
45. M. AREFI, A.H. SOLTAN-ARANI, *Higher order shear deformation bending results of a magneto-electrothermoelastic functionally graded nanobeam in thermal, mechanical, electrical, and magnetic environments*, Mechanics Based Design of Structures and Machines, **46**, 6, 669–692, 2018.
46. F. EBRAHIMI, M.R. BARATI, *Thermal environment effects on wave dispersion behavior of inhomogeneous strain gradient nanobeams based on higher order refined beam theory*, Journal of Thermal Stresses, **39**, 12, 1560–1571, 2016.
47. M. GHADIRI, A. JAFARI, *Thermo-mechanical analysis of FG nanobeam with attached tip mass: an exact solution*, Applied Physics A, **122**, 1–13, 2016.
48. F. EBRAHIMI, M.R. BARATI, *Vibration analysis of viscoelastic inhomogeneous nanobeams resting on a viscoelastic foundation based on nonlocal strain gradient theory incorporating surface and thermal effects*, Acta Mechanica, **228**, 1197–1210, 2017.
49. F. EBRAHIMI, M.R. BARATI, *Small-scale effects on hygro-thermo-mechanical vibration of temperature-dependent nonhomogeneous nanoscale beams*, Mechanics of Advanced Materials and Structures, **24**, 11, 924–936, 2017.
50. S.A. HOSSEINI, O. RAHMANI, S. BAYAT, *Thermal effect on forced vibration analysis of FG nanobeam subjected to moving load by Laplace transform method*, Mechanics Based Design of Structures and Machines, **51**, 7, 3803–3822, 2023.

51. F. EBRAHIMI, E. SALARI, S.A.H. HOSSEINI, *Thermomechanical vibration behavior of FG nanobeams subjected to linear and non-linear temperature distributions*, Journal of Thermal Stresses, **38**, 12, 1360–1386, 2015.
52. Z. LV, H. LIU, *Uncertainty modeling for vibration and buckling behaviors of functionally graded nanobeams in thermal environment*, Composite Structures, **184**, 1165–1176, 2018.
53. M.A. ALAZWARI, I. ESEN, A.A. ABDELRAHMAN, A.M. ABDRABOH, M.A. ELTAHER, *Dynamic analysis of functionally graded (FG) nonlocal strain gradient nanobeams under thermo-magnetic fields and moving load*, Advances in Nano Research, **12**, 3, 231–251, 2022.
54. B.V. TUYEN, N.D. DU, *Analytic solutions for static bending and free vibration analysis of FG nanobeams in thermal environment*, Journal of Thermal Stresses, **46**, 9, 871–894, 2023.
55. A.M. SHAJAN, K. SIVADAS, R. PISKA, C. PARIMI, *Hygrothermal effects on vibration response of porous FG nanobeams using nonlocal strain gradient theory considering thickness effect*, International Journal of Structural Stability and Dynamics, **23**, 2440016, 2023.
56. F. FAN, B. LEI, S. SAHMANI, B. SAFAEI, *On the surface elastic-based shear buckling characteristics of functionally graded composite skew nanoplates*, Thin-Walled Structures, **154**, 106841, 2020.
57. S. SAHMANI, A.M. FATTAHI, N.A. AHMED, *Surface elastic shell model for nonlinear primary resonant dynamics of FG porous nanoshells incorporating modal interactions*, International Journal of Mechanical Sciences, **165**, 105203, 2020.
58. K.K. ŽUR, S.A. FAGHIDIAN, *Analytical and meshless numerical approaches to unified gradient elasticity theory*, Engineering Analysis with Boundary Elements, **130**, 238–248, 2021.
59. Y.S. TOULOUKIAN, *Thermophysical Properties of High Temperature Solid Materials*, Vol. 3: *Ferrous Alloys*, Macmillan, New York, 1967.
60. T.K. NGUYEN, B.D. NGUYEN, T. VO, H.T. THAI, *Hygro-thermal effects on vibration and thermal buckling behaviours of functionally graded beams*, Composite Structures, **176**, 1050–1060, 2017.
61. V.T. GRANIK, M. FERRARI, *Microstructural mechanics of granular media*, Mechanics of Materials, **15**, 4, 301–322, 1993.
62. U. GUL, M. AYDOGDU, G. GAYGUSUZOGLU, *Axial dynamics of a nanorod embedded in an elastic medium using doublet mechanics*, Composite Structures, **160**, 1268–1278, 2017.
63. U. GUL, M. AYDOGDU, *Structural modelling of nanorods and nanobeams using doublet mechanics theory*, International Journal of Mechanics and Materials in Design, **14**, 195–212, 2018.
64. U. GUL, M. AYDOGDU, G. GAYGUSUZOGLU, *Vibration and buckling analysis of nanotubes (nanofibers) embedded in an elastic medium using Doublet Mechanics*, Journal of Engineering Mathematics, **109**, 85–111, 2018.

Received May 13, 2024; revised version September 9, 2024.

Published online October 28, 2024.
